2022

Optimal Design of Photovoltaic, Biomass, Fuel Cell, Hydrogen Tank units and Electrolyzer hybrid system for a remote area in Egypt

Hoda Abd El-Sattar
Aswan University, Egypt

Salah Kamel
Aswan University, Egypt

Hamdy M. Sultan
Minia University, Egypt

See next page for additional authors

Authors

Hoda Abd El-Sattar, Salah Kamel, Hamdy M. Sultan, Hossam Zawbaa, and Francisco Jurado
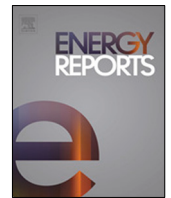
Research paper

Optimal design of Photovoltaic, Biomass, Fuel Cell, Hydrogen Tank units and Electrolyzer hybrid system for a remote area in Egypt

Hoda Abd El-Sattar [a,b], Salah Kamel [a], Hamdy M. Sultan [c], Hossam M. Zawbaa [d,e,*], Francisco Jurado [b]

[a] Department of Electrical Engineering, Faculty of Engineering, Aswan University, 81542 Aswan, Egypt
[b] Department of Electrical Engineering, University of Jaén, 23700 EPS Linares, Jaén, Spain
[c] Electrical Engineering Department, Faculty of Engineering, Minia University, 61111 Minia, Egypt
[d] Faculty of Computers and Artificial Intelligence, Beni-Suef University, Beni-Suef, Egypt
[e] Technological University Dublin, Dublin, Ireland

ARTICLE INFO

ABSTRACT

In this paper, a new isolated hybrid system is simulated and analyzed to obtain the optimal sizing and meet the electricity demand with cost improvement for servicing a small remote area with a peak load of 420 kW. The major configuration of this hybrid system is Photovoltaic (PV) modules, Biomass gasifier (BG), Electrolyzer units, Hydrogen Tank units (HT), and Fuel Cell (FC) system. A recent optimization algorithm, namely Mayfly Optimization Algorithm (MOA) is utilized to ensure that all load demand is met at the lowest energy cost (EC) and minimize the greenhouse gas (GHG) emissions of the proposed system. The MOA is selected as it collects the main merits of swarm intelligence and evolutionary algorithms; hence it has good convergence characteristics. To ensure the superiority of the selected MOA, the obtained results are compared with other well-known optimization algorithms, namely Sooty Tern Optimization Algorithm (STOA), Whale Optimization Algorithm (WOA), and Sine Cosine Algorithm (SCA). The results reveal that the suggested MOA achieves the best system design, achieving a stable convergence characteristic after 44 iterations. MOA yielded the best EC with 0.2106533 \$/kWh, the net present cost (NPC) with 6,170,134 \$, the loss of power supply probability (LPSP) with 0.05993%, and GHG with 792.534 t/y.

1. Introduction

1.1. Motivations

Energy is more than just producing electricity; it is an economic pillar and a source of long-term prosperity. Renewable energy utilization is still not growing at the desired rate. The total share of renewable energy in global electricity production has not exceeded more than 27% (Anon, 2021f). This indicates that fossil energy is still dominant in energy production, and the reason can be attributed to the fact that generating renewable energy is still relatively expensive. However, it is planned that by the year 2030, renewable energy sources, which include hydropower, wind energy, solar photovoltaic energy, bio-energy, geothermal energy, and marine energy, will contribute approximately 40% of the electricity supply (Anon, 2021g).

Egypt is one of the countries that is working to promote the use of renewable energy sources by exploiting all available resources to optimize the efficient use of various renewable sources and developing their technology to contribute to economic growth and environmental preservation (El-Sattar et al., 2016). A strategy has been developed that includes increasing the contribution of renewable energy by 20% and 42% of electric energy production by 2022 and 2035, respectively (Anon, 2021e). The objective of this strategy is to provide the necessary energy supplies for development needs, including identifying the optimal mix of energy, developing reliance on renewable sources and raising the efficiency of its use (Anon, 2021d). According to the data from International Renewable Energy Agency (IRENA) in 2018, Fig. 1 presented the renewable sources generation statues (GWh) in Egypt.

Egypt is one of the wealthiest countries in the world in the field of solar energy and bioenergy due to its geographical location and the availability of raw materials for biomass, especially from crop wastes. For the solar energy field, Egypt enjoys direct

* Correspondence to: Technological University Dublin, Park House, 191 N Circular Rd, Cabra East, Grangegorman, Dublin, D07 EWV4, Ireland.
E-mail addresses: eng_ha20@yahoo.com (H.A. El-Sattar), skamel@aswu.edu.eg (S. Kamel), hamdy.soltan@mu.edu.eg (H.M. Sultan), hossam.zawbaa@gmail.com (H.M. Zawbaa), fjurado@ujaen.es (F. Jurado).

Nomenclature

ABC	Artificial Bee Colony Algorithm
ACO	Ant colony optimization algorithm
AEFO	Artificial Electric Field optimizer
AEO	Artificial Ecosystem Optimization
BA	Bees algorithm
BG	Biomass Gasifier
BSA	Backtracking Search Algorithm
CRF	Capital Recovery Factor
CS	Cuckoo Search Algorithm
DF	Dragonfly Optimizer Algorithm
DG	Diesel Generator
DSPBO	Enhanced model of the Student Psychology Based Optimizer
EC	Energy Cost
EO	Equilibrium Optimizer
FC	Fuel Cell
FFA	Firefly algorithm
FOA	Firefly Optimization Algorithm
FPA	Flower Pollination Algorithm
GA	Genetic Algorithm
GHG	Greenhouse Gas emissions
GWO	Grey Wolf Optimizer
GWP	Global Warming Potential
HHO	Harris Hawks optimizer
HSA	Harmony search algorithm
HT	Hydrogen Tank units
IACO	Improved ant colony optimization algorithm
IAEO	Improved Artificial Ecosystem Optimization
IRENA	International Renewable Energy Agency
IWO	Invasive weed optimization
JOA	Jaya Optimization Algorithm
LPSP	Loss of Power Supply Probability
MBA	Mine Blast Algorithm
MFO	Moth–Flame Optimizer
MOA	Mayfly Optimization Algorithm
MOCSA	multi-objective crow search algorithm
NPC	Net Present Cost
NSGAII	Non-dominated sorting genetic algorithm
PSO	Particle Swarm Optimizer
PSOGSA	Hybrid particle swarm-gravitational search Algorithm
PV	Photovoltaic
SA	simulated annealing
SAA	Simulated annealing algorithm
SCA	Sine Cosine Algorithm
SPEA2	Strength Pareto Evolutionary Algorithm 2
SSA	Salp Swarm Algorithm
SSO	Social Spider Optimizer
STOA	Sooty Tern Optimization Algorithm
TAC	total annual cost
TLBO	Teaching–Learning Based Optimization
WCA	Water Cycle Algorithm
WOA	Whale Optimization Algorithm
WTs	Wind Turbines

Symbols

BE_T	Total biomass consumption (kWh)
$BG_P(t)$	Generator output power (kW)
$B_{rated}(t)$	Biomass consumption rate per hour
$C_{A\_Cap}^y$	Annual interest of the capital cost for each unit
C_{A_fuel}	Annual fuel cost of the biomass unite
$C_{A\_Rep}^y$	Replacement cost for each unit
C_A^y	Annualized cost of each subsystem component
C_B	A uniformly distributed arbitrary coefficient
C_f	The controlling coefficient that decreases from C_f to zero
C_i	The location of the search agent in STOA
CO_2	Carbon Dioxide
C_{OM}^y	Operation and maintenance cost of each unit
CRF^y	The Capital Recovery Factor of the required unit
$C_{I\_Cap}^y$	The initial capital cost of the required unit
c_ω	The walk coefficient
D_A	The movement of the sooty tern in the search field
E_{Con}	Energy consumption (kWh)
F_0	No-load fuel consumption (kg/h/50 Kw)
$F_{BG}(t)$	Average fuel consumption per hour
FC_P	Generated electrical power from FC (kW)
FC_P^{max}	The maximum rating of the FC unit
F_m	Marginal fuel consumption (kg/h/50 kW)
G_i	The distance between the search agent and the best one
G_N	Number of biomass generators
G_N^{max}	The maximum number of gasifier generators
GP_{rat}	Generator rated power (kW)
HHV_H	Higher heat value of the stored hydrogen (kWh/kg)
HT_m	Stored hydrogen mass in the HT (kg)
HT_m^{max}	The maximum capacity of the HT in kg.
HT_E	Stored hydrogen energy (kWh)
k_1 and k_2	Attraction constants for evaluating the cognitive and social behaviors
LHV_B	Feedstock lower heat value (MJ/kg)
LHV_{sy}	Syngas lower heat value (MJ/kg)
$Load_P$	The load power (kWh)
Max_{it}	The maximum iterations number
m_B	Feedstock mass flow (kg/h)
m_{sy}	Syngas mass flow (kg/h)
$P_{ELE/HT}$	Rated power of water electrolyzer
$pbest_{ij}$	The best position reached by the ith mayfly in the ith dimension

P_{Dum}	Dummy load
$P_{ELE/HT}^{max}$	The maximum rating of the electrolyzer unit
P_{EXC}	Excess energy
P_{EXE}^{max}	The maximum rating of the excess energy
$P_{HT/FC}$	Power supplied from the HT to the FC
$p_i(t)$	the current iteration (t)
P_i^{it}	The best individual's position in SCA
p_{ij}	The location of the ith search agent in the jth dimension
P_{ren}	Generated power from renewable sources
$P_{ren/ELE}$	Electrical energy from renewable sources feeding the electrolyzer
PV_N	Number of PV units
PV_N^{max}	The maximum number of PV modules
PV_P	Generated power of the PV (kWh)
PV_P^{rat}	PV Rated Power (kW)
PV_η	PV module efficiency
$q_i(t)$	The position of a certain individual female mayfly in the search area
$q_{ij}(t)$	The location of the ith female in the jth dimension during the iteration t
$r_1, r_2, r_3,$ and r_4	The four random control parameters used to prevent becoming stuck in poor solutions and keep the exploration and exploitation processes in balance
r_{fm}	The distance between the male and female mayflies
r_g	The distance between the position of the individual in the $p_i(t)$ and its gbest
R_i	The various positions of the search agent $X_i(it)$ in the search space in its movement towards the best fittest sooty tern
r_p	the distance between the position of the individual in the $p_i(t)$ and its pbest
$SR_{int}(t)$	Solar Radiation Intensity at a time (t) (kWh/m^2)
T_A	Ambient temperature (°C)
T_C	Cell Temperature (°C)
T_{nor}	Cell temperature at normal operating conditions (°C)
T_r	Reference cell temperature (°C)
$u_{ij}(t)$	The velocity of the ith female mayfly in the jth dimension
v_{ij}	The velocity of the ith search agent in the jth dimension
W_η	Wiring Efficiency
$x', y',$ and $z',$	The angle of attack
X_{best}	Best search agent
$X_i(it)$	The current location of the sooty tern at the it-th iteration
X_i^{it}	The current individual (i) at iteration (it) in SCA
δ_T	Temperature coefficient of maximum power (°C^{-1})

|	
η_{ELE}	Electrolyzer efficiency
η_{FC}	FC overall efficiency
η_{HT}	HT efficiency
η_{inv}	Inverter efficiency
η_{sy}	Syngas efficiency (%)
c	A coefficient describing the nuptial dancing of the mayflies.
f(.)	The objective function of the optimization problem
gbest	The global best position
i	the position of certain mayfly
m	A variable that ranges between ($0 \le k \le 2\pi$)
p	The position vector
pbest	The best position
Radius	The radius of each turn in the spiral
u and v	Factors describing the spiral shape
v	The velocity vector
X	The control variables of the optimization problem
β	The weight factor value of each objective function
Δt	Time durations during simulation
ε	A random number in the range of $[-1, 1]$
λ	Limit the visibility between individual mayflies
ρ	Random numbers in Gauss distribution
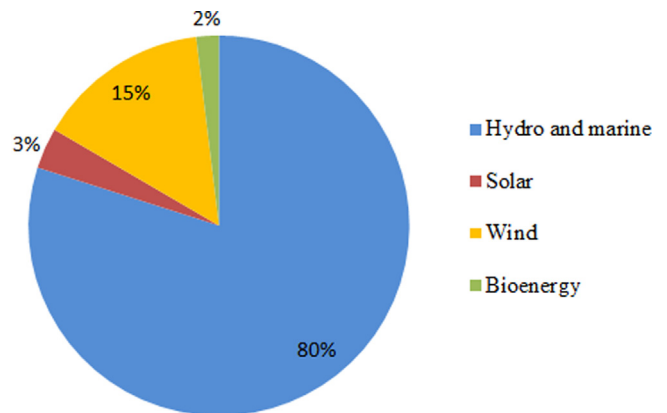
Fig. 1. The status of renewable sources generation in Egypt.

solar radiation with an intensity that varies from 2000 to 3200 kWh/m^2/year from north to south (Anon, 2021b). The average daily sunshine ranges between 9 to 11 hours/day from North to South (Anon, 2021b,a). Currently, solar energy projects in Egypt have become one of the strategic axes of the plan to expand reliance on renewable energy. Solar energy represented about 2% of the total energy generated in Egypt from 2012 to 2017 (Anon, 2021b). During 2019–2020, the electricity generated through solar energy reached about 3655 GWh (Anon, 2021d).

Bioenergy is the energy produced from organic materials in which energy is stored. The most important sources are agricultural waste, food waste, and livestock dung (El-Sattar et al., 2020b). Egypt has a huge potential for bioenergy production, especially from the crop remains, as about 21 million tons of

Table 1

A summary of different hybrid system configurations.

Hybrid System Configuration	Ref.	Location	Technique	Objective function
PV, WTs, DG, and batteries	Diab et al. (2019)	Abu-Monqar village in the Western Desert of Egypt	WOA, WCA, PSOGSA, MFO	EC LPSP
	Fathy et al. (2020)	A remote area in Aljouf region in the north of Saudi Arabia	SSO, HHO, GWO, MVO, ALO	EC
	Kharrich et al. (2021a)	Dakhla area in Morocco	EO, HHO, AEFO, GWO, STOA	NPC
	Suresh and Meenakumari (2019)	–	An improved GA	EC, NPC, LPSP, CO_2 emissions
	Kharrich et al. (2021b)	Rabat, Morocco	MOPSO, PESA II, SPEA2	Total NPC, CO_2 emission
PV, WTs, and batteries	Naderipour et al. (2019)	Ahvaz city in Iran	GWO and PSO	NPC
	Sanajaoba (2019)	Manipur state in India	FOA	EC
PV, WTs, BG, and batteries	Tabak et al. (2019)	a faculty building in Karabük University campus, Turkey	GWO, GA, and SA	Total NPC, LPSP, and EC
	Alshammari and Asumadu (2020)	A small rural community located at latitude 29° 49.794′ N and longitude 39° 34.362′ E	HSA, JOA, and PSO	lower cost and reduce CO_2 emission
PV, BG, and battery	Singh and Kaushik (2016)	–	ABC and HOMER	annual cost
	Ghosh and Karar (2018)	Kaidupur village, in Punjab State, India	DF and ABC	TAC
	Eteiba et al. (2018)	Monshaet Taher village in Beni Suef, Egypt	FPA, HS, ABC, and FOA	NPC
PV, WTs, BG, and pumped hydro storage	Alturki and Awwad (2021)	Saudi Arabia	WOA, FFA, and PSO	EC
PV, Biogas generator, Battery, and Pumped-storage hydro	Das et al. (2019)	A radio transmitter station in India	WCA and MFO	Total NPC
	Shi et al. (2021)	A radio transmitter station in China at Hubei's Three Gorges Dam	DSPBO, WCA, MOA, GA, FOA, and GWO	Reducing the overall life cycle cost

agricultural waste are disposed of annually (Hassan et al., 2014). This waste can be exploited and invested well in the bio-economy by using appropriate technologies.

1.2. Literature review

Currently, there are many papers related to studying the performance of hybrid renewable energy systems and studying different optimization algorithms. The purpose of such studies is to assess the system components' maximum capacity and improve the main economic and technical indicators in the design of these systems. In Naderipour et al. (2019), the Grey Wolf Optimizer (GWO) has been applied to reduce the total net present cost (NPC) by considering the reliability constraints for an isolated hybrid system in Ahvaz city in Iran. This research is based on studying three different system configurations; the first combination consists of PV panels, wind turbines (WTs), and batteries, the second one consists of PV, and batteries, and the third consists of WTs, and batteries. The obtained results from the proposed GWO are compared with the particle swarm Optimizer (PSO). The obtained results showed the effectiveness of the proposed GWO in designing a reliable and costless PV, WTs, and batteries hybrid system.

As is evident, most of the papers are concerned with studying hybrid systems consisting of PV, WTs, and DG with batteries. Many researchers have currently studied the optimal sizing of the hybrid system consisting of biomass generators (BG) with the PV and WTs using different optimization algorithms. HOMER software is often used in simulating and analyzing the hybrid power system from a techno-economic perspective. In Cano et al. (2020), the authors proposed an optimal configuration analysis using HOMER software for an off-grid hybrid system based on PV, BG, hydrokinetic turbines, and batteries banks located in southern Ecuador. Also, in Li et al. (2020), HOMER has been applied to

perform the techno-economic analysis of a stand-alone hybrid system located in a remote village in west China. The proposed system consists of PV, WTs, BG, and batteries.

Based on the Literature review, Table 1 provides a summary of these cited references depending on their studied systems' configurations. At the same time, a summary of some recent hybrid system research based on FC configuration is presented in Table 2.

This paper focuses on studying the optimal sizing of an isolated hybrid system based on PV, BG, Electrolyzer units, HT units, and FC to serve a remote area Abu-Monqar in the Western Desert of Egypt. The literature works demonstrate that metaheuristic algorithms based on natural strategies have been successfully applied to a variety of optimization issues. According to the principle of "no free lunch" (NFL) (Wolpert and Macready, 1997), which can be characterized as "no optimization approach offers good performance for free". This principle supports the argument that existing techniques can still be improved, and new ones can be implemented. Based on the previous context, MOA has been applied for solving the optimization problem related to the suggested configuration. The suggested population-based approach is inspired by adult mayfly behavior, such as crossover, mutation, swarm gathering, nuptial dance, and random walk; these behaviors incorporate significant benefits of the proposed algorithm, which improve exploration. To estimate the effectiveness of this algorithm and to test the characteristics of exploitation and exploration of the MOA method; a qualitative analysis has been made, in which this method has been benchmarked against seven high-quality meta-heuristic optimization algorithms on 25 test functions which are classified in 3 groups (unimodal, multimodal and fixed-dimension), as well as 13 CEC2017 test functions, multi-objective optimization, and a discrete classic flow-shop scheduling problem. Also, it has been compared with other popular metaheuristic algorithms, specifically PSO, GA, FOA, DE,

Table 2
FC based on different hybrid energy systems.

Ref.	Hybrid System Configuration	Location	Technique	Objective function	Findings
Maleki and Pourfayaz (2015)	PV/WTs/DG/battery PV/WTs/DG/FC	Iran	HSA HOMER SAA	TAC	The PV/WT/DG/battery system is more cost-effective than the PV/WT/DG/FC system. Nonetheless, using PV/WT/DG/FC as an energy source provides a reliable energy source, and with improved FC and electrolyzer efficiency, may become economically competitive in the future.
Sultan et al. (2021)	PV/WTs/FC	Suez Gulf in Egypt	IAEO,AEO PSO, SSA, and GWO	EC	The suggested IAEO algorithm shows quick convergence properties, the best objective function minimum values, and the lowest EC compared to the traditional AEO, PSO, SSA, and GWO algorithms.
Dong et al. (2016)	PV/WTs/battery/HT	Zhejiang in China	IACO ACO	Annual Cost LPSP	The hybrid system described in this study is based on the hybrid system of battery and hydrogen. Under certain constraints, the results of IACO algorithm presented that the suggested hybrid system is more cost-effective than others because of battery leakage and lower FC efficiency.
Attemene et al. (2020)	WT/FC/battery/super-capacitor	Tanda in Ivory Coast	NSGAII	TAC LPSP	This study aims to figure out which variables had the biggest influence. The most influential parameters were the wind speed profile, wind generator cost, FC cost, and battery cost. As a result, the suggested design would be quite beneficial in places with high wind potential.
Khan and Javaid (2020)	PV/WT/FC PV/FC WT/FC	Hawksbayin Pakistan	JOA GA, BSA and PSO	TAC	The PV/FC is the most cost-effective hybrid system compared to the PV/WT/FC and WT/FC systems. The Jaya method's results showed its superiority compared to other algorithms used.
Duman and Güler (2018)	PV/WT/FC	Turkey	HOMER	EC	This system presented the dispatch control strategies and the optimal ratings of the renewable system units. According to the techno economic analysis of this study, showed that battery storage is still economically superior to hydrogen storage.
Jamshidi and Askarzadeh (2019)	PV/DG/FC (off-grid)	Kerman in Iran	MOCSA	NPC LPSP	According to the design results, incorporating hydrogen energy technology will decrease the total cost of hybrid energy systems. Furthermore, operating reserve has a greater impact on the Pareto front than load and solar power uncertainties.
Gharibi and Askarzadeh (2019)	PV/DG/FC (grid-connected)	Kerman in Iran	MOCSA	EC LPSP	Based on the design results, when the price of electricity reduces, the EC rises and the value of the grid factor decrease.
Fathy (2016)	PV/WT/FC	Egypt	MBA, PSO ABC, and CS	Annual Cost	The proposed algorithm based on MBA showed its effective for solving the presented optimization problem of optimal sizing of the hybrid PV/WT/FC system compared to the other three algorithms used.
Hadidian Moghaddam et al. (2019)	PV/WT/FC PV/FC WT/FC	Iran	FPA PSO TLBO	Total NPC	FPA method showed the best results in solving the optimal sizing problem with fast convergence, minimum Total NPC and better reliability compared to the other optimization algorithms used. PV/WT/FC system is the most cost-effective for many situations, with lower costs and higher reliability indices in comparison to other suggested hybrid system combinations.

HS, invasive weed optimization (IWO), and bees algorithm (BA), under the same conditions to achieve fairness in comparison. The obtained results demonstrate that the proposed MOA has superior performance in convergence rate compared to the other well-known metaheuristic optimization which has been used in this paper. The suggested MOA method's convergence characteristic is noteworthy since it frequently achieves the best overall solution in the early iterations. MOA's findings are satisfactory for discrete and multi-objective optimization problems. To the authors' knowledge, MOA has never been used before to evaluate the optimal size for the proposed configuration system. In Chen et al. (2021), MOA has been adopted for analyzing the optimal allocation with the minimum installation cost for an Electric Vehicle Charging Station system in India.

1.3. Contribution and paper organization

The novelty of this work consists in studying and providing the optimal sizing and energy management strategy of integrating an isolated hybrid system based on PV, BG, Electrolyzer units, HT units, and FC to serve a rural town called Abu-Monqar in the Western Desert of Egypt. The MOA technique was developed with Matlab© and applied to solve the optimization problem related to the suggested configuration. According to (Zervoudakis and Tsafarakis, 2020), the suggested MOA is a new optimization method, and it incorporates the best features of PSO, GA, and FOA. MOA can be considered a modification of PSO; it provides a powerful hybrid algorithmic structure based on mayfly behavior for researchers attempting to improve PSO performance using crossover and local search techniques. The major contributions of this study can be summarized as follows;
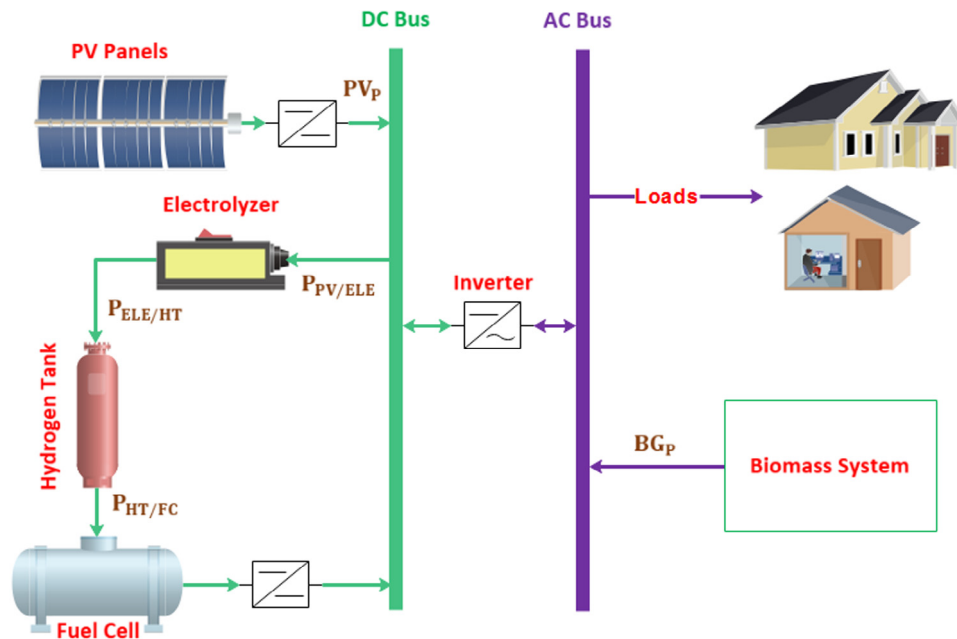
Fig. 2. The proposed hybrid system's configuration layout.

- A new hybrid energy system, consisting of PV, BG, FC, Electrolyzer units, and HT units, has been developed for a small village located in the Western Desert of Egypt;
- The optimal size of the proposed stand-alone hybrid system is determined using a novel MOA approach;
- To prove the optimal effective and performance of the MOA methodology, the results of MOA are compared with a three optimization algorithms; STOA (Maleki et al., 2020), WOA (Bukar et al., 2019), and SCA (Sultan et al., 2020);
- The optimal function of this hybrid system is to minimize the EC and reduce the CO_2 emissions;
- Evaluate the optimal decision variables of the components, which include the number of PV units (PV_N), number of biomass generators (G_N), the rated power of the FC (FC_P), the rated power of the water electrolyzer ($P_{ELE/HT}$), and the mass of the hydrogen gas tank (HT_m).

The organization of the rest of the paper is as follows: Section 2 provides the construction of the hybrid system, which consists of PV, BG, Inverter, FC, Electrolyzer units, and HT components. Section 3 discusses the formulation of the optimization problem, which includes the economic and cost analysis, objective function, constraints, and operation strategy. Section 4 describes the proposed optimization of MOA, STOA, WOA and SCA algorithms; Section 5 presents the results and discussion, which includes the meteorology of the case study area and the discussion of the optimal results, while Section 6 provides the conclusion of this study.

2. The construction of the proposed hybrid system

In this section, the stand-alone configuration of PV, BG, Inverter, FC, Electrolyzer units, and HT components is discussed in detail. Fig. 2 illustrates the graphical diagram of the proposed hybrid energy system. PV units, electrolyzer, and FC are connected to the DC bus, where the PV modules provide the required input power to the electrolyzer. The biomass plant is connected to the AC bus, to which the main load is connected. The generated power from the PV and FC systems is converted through DC/AC inverter to meet the demand load. The parameters and operating characteristics of all system components are presented in Table 3.

The control diagram of the proposed hybrid system is shown in Fig. 3. This figure illustrates a general scheme of the system's operation. If the energy produced from the PV and BG units covers the load needed power, then no power from the FC is needed, and no power is supplied to the electrolyzer unit. If the energy produced exceeds the load needed, in this case, this excess energy will feed the electrolyzer and begin producing hydrogen, which is used to charge the HT units. If the HT becomes full, the dummy load will consume this excess power. If the energy generated by the PV and BG units is unable to fulfill the load power needs, the FC will utilize hydrogen stored in the HT units to compensate for the power generation shortfall.

2.1. Photovoltaic solar module (PV)

PV module is a device that uses the photoelectric effect to transform light energy directly into electrical energy. It is a simple energy provider since it does not require chemical reactions or fuel to generate electrical energy. (Singh and Baredar, 2016). The generated power of the PV array (PV_P) and the cell temperature (T_C) can be evaluated according to the following equations (Geleta et al., 2020; Maleki et al., 2020; Bukar et al., 2019; Sultan et al., 2020):

$$PV_P(t) = \left(\frac{SR_{int}(t)}{1000} \right) \left(PV_N PV_P^{rat} W_\eta PV_\eta \right) (1 - \delta_T(T_C - T_r)), \quad (1)$$

$$T_C(t) = SR_{int}(t) \left(\frac{T_{nor} - 20}{800} \right) + T_A, \quad (2)$$

where $SR_{int}(t)$, PV_N, PV_P^{rat}, W_η, and PV_η are the intensity of solar radiation at a time (t), the number of PV units, the rated power, the wiring efficiency, and the PV module efficiency, respectively, δ_T denotes the PV module temperature coefficient of maximum power, T_A is the ambient temperature, and T_r denotes the reference temperature of the solar cell is equal to 25 °C. T_{nor} is the cell temperature at normal operating conditions, it is dependent on four basic standard reference settings; solar irradiation with 800W/m², wind velocity with 1 m/s, air temperature of 20 °C, and inclination angle of 45° from the horizontal (Anoune et al., 2020).
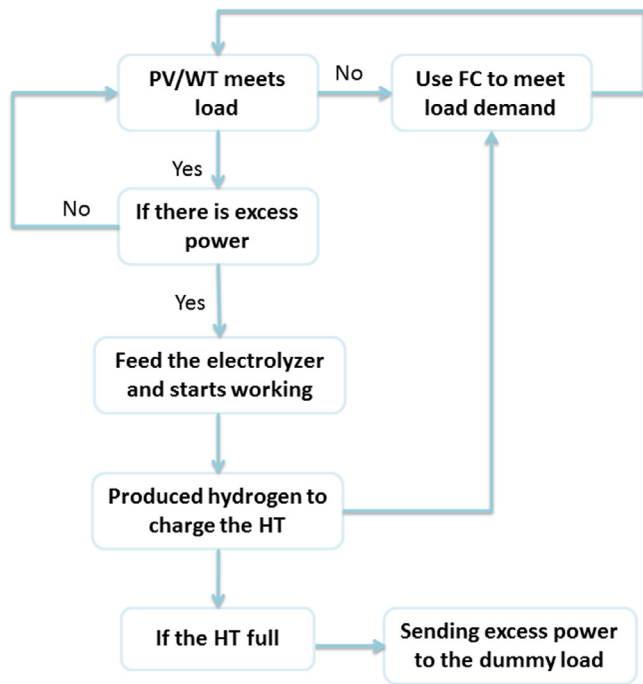
Fig. 3. The control diagram of the proposed hybrid system.

2.2. Biomass system modeling

This work uses a small-scale downdraft gasification technology that converts solid biomass into a gaseous fuel (syngas) used in turbines to generate electricity. The reason for choosing downdraft gasification technology is that the fixed bed gasifiers are often simple and low-cost, and it has a high total carbon conversion rate and high solids residence time and low gas velocity. A downdraft gasifier is a co-current reactor in which the gasification agent is supplied from the top or sides of the reactor, causing the feed stock and gasification agent to flow in the same direction. Downdraft gasifiers are commonly utilized in engine applications because of their simplicity, low investment costs, good product gas quality, and ability to install in small spaces.

Egypt is one of the agricultural countries, which means the availability of agricultural residues that can be used as biomass feedstock. Egypt produces the largest amount of corn crop residues annually compared to other agricultural residues, with a total amount of 3.23 million tons/year (Abdelhady et al., 2021). Corn stalk is one of the feed stocks with the greatest potential for energy production and industrial applications because of its abundance, which is abundant in the middle region of Egypt. In this study, corn stalk is used due to its availability in areas near the study case area. In addition, compared to other agricultural crop wastes, corn stalk is a possible hydrocarbon feedstock for biomass gasification since it contains substantial amounts of carbon and modest levels of ash and sulphur.

Based on the features of the corn stalk used, the system performance is expressed as follows (Cano et al., 2020; Eteiba et al., 2018; El-Sattar et al., 2018):

$$\eta_{sy} = \frac{LHV_{sy}m_{sy}}{LHV_{B}m_{B}}, \tag{3}$$

$$BG_P(t) = \frac{G_N}{F_m}\left(\frac{\eta_{sy} \, LHV_B B_{rated}(t)}{LHV_{sy}} - F_0 GP_{rat}\right), \tag{4}$$

$$F_{BG}(t) = \frac{LHV_{sy}}{\eta_{sy} LHV_B}\left(G_N F_0 GP_{rat} + F_m BG_P(t)\right), \tag{5}$$

Where η_{sy} denotes the syngas efficiency. LHV_{sy} and LHV_B are the lower heat value of the syngas and biomass feedstock, respectively. m_{sy} and m_B are the mass flow of the syngas and the biomass feedstock, respectively. $BG_P(t)$, G_N, $B_{rated}(t)$, GP_{rat}, $F_{BG}(t)$, F_m, and F_0 are the output power of the generator, the number of generators used, the biomass consumption rate per hour, the generator rated power, average fuel consumption per hour, Marginal and No-load fuel consumption, respectively.

Greenhouse Gas (GHG) emissions from the feedstock residues are calculated as (Eteiba et al., 2018):

$$BE_T = LHV_B * Sum(B_{rated}), \tag{6}$$

$$E_{Con} = BE_T * 0.0002778, \tag{7}$$

$$GHG = E_{Con} * GWP * 0.43, \tag{8}$$

Where BE_T and E_{Con} are the total biomass consumption and the energy consumption (kWh), respectively. GWP is the global warming potential (=1) (Sultan et al., 2021), and 0.43 is the electricity emission factor (kg CO_2/kWh) (Ray et al., 2007).

2.3. Electrolyzer modeling

The electrolyzer consists of an anode and a cathode separated by an electrolyte in which an electric current passes through, creating a chemical reaction that decomposes water into its two elements (hydrogen and oxygen). The generated hydrogen is collected around the surface of the anode. Based on (Kashefi Kaviani et al., 2009), most of the electrolyzers, produce hydrogen at 30 bar but this hydrogen is transferred directly to the FC at a low pressure of 1.2 bar. In most research, the produced hydrogen is directly delivered to the hydrogen tank, however, in other studies, the pressure is raised to 200 bar with the use of a compressor in order to increase the stored energy in the tank (Kashefi Kaviani et al., 2009). Other works employ two tanks with low and high pressure. If this tank is fully charged, a compressor is used to transport the hydrogen to the high-pressure tank in order to waste as little energy as possible because the compressor will not be running all the time (Mills and Al-Hallaj, 2004). In this study, Proton-conducting polymeric membrane electrolyzer (PEM) is used, where the produced hydrogen of the electrolyzer is immediately transported to the hydrogen tank at a pressure of 30 bar. The energy is transferred to the hydrogen tank from the electrolyzer ($P_{ELE/HT}$) is expressed as (Sultan et al., 2021; Kashefi Kaviani et al., 2009);

$$P_{ELE/HT} = \eta_{ELE}*P_{ren/ELE}, \tag{9}$$

Where η_{ELE} denotes the efficiency of an electrolyzer and $P_{ren/ELE}$ represents the electrical energy feeding the electrolyzer from renewable sources.

2.4. Hydrogen tank storage (HT)

After the hydrogen and oxygen separation process, the hydrogen gas is transported and stored in HT to be used in the FC for power generation. To ensure the process balance, the HT upper pressure is adjusted to the same as that of the water electrolyzer pressure, while the HT lowest pressure is adjusted to the same fuel cell pressure (Attemene et al., 2020). During the operation, the stored hydrogen mass in the HT (HT_m) is constrained by the minimum and maximum values (Sultan et al., 2021) according to this formulation:

$$HT_m^{min} \leq HT_m(t) \leq HT_m^{max}, \tag{10}$$

Table 3
Main parameters of the stand-alone hybrid system PV/Biomass/FC.

Component	Parameter	Value	Unit
PV System (Diab et al., 2019; Sultan et al., 2021)	PV module capital cost	7000	$
	δ_T	0.0037	–
	PV_η	15	%
	T_r	25	°C
	Rated power	1	kW
	Length	1625	Mm
	Width	1019	Mm
	Thickness	46	Mm
	lifetime of PV system	20	Year
	PV replacement cost	13885	$
	O&M cost	20	$/unit-year
Inverter Unit (Sultan et al., 2021)	η_{inv}	95	%
	Max. power	1	kW
	inverter lifespan	15	Year
	Inverter Capital Cost	800	$/unit
	Replacement cost	750	$/kw
	O&M cost	8	$/unit-year
Gasification System	LHV$_B$ (El-Sattar et al., 2018)	14.8	MJ/kg
	LHV$_{sy}$ (El-Sattar et al., 2018)	4.766	MJ/kg
	η_{sy}	80	%
	GP$_{rat}$	40	KW
	No-load fuel consumption (F_0) (Eteiba et al., 2018)	0.0644	kg/h/50 kW
	Marginal fuel consumption (F_m) (Eteiba et al., 2018)	0.2998	kg/h/50 kW
	Capital Cost (Alturki and Awwad, 2021)	23,700	$/kw
	Lifespan (Alturki and Awwad, 2021)	15,000	h
	Replacement cost (Alturki and Awwad, 2021)	15000	$/unit
	Yearly O&M cost (Alturki and Awwad, 2021)	0.05	$/h
Electrolyzer Unit (Sultan et al., 2021)	Rated Power	1	kW
	Lifespan	20	Year
	Efficiency	75	%
	Capital cost	2000	$/unit
	Replacement cost	1500	$/unit
	Yearly O&M cost	25	$/unit
Hydrogen Tank Unit (Sultan et al., 2021)	Power	1	kW
	Efficiency	95	%
	Capital cost	1300	$/unit
	O&M cost	15	$/unit-year
	Replacement cost	1200	$/unit
	Lifespan	20	Year
FC System (Sultan et al., 2021)	Power	1	kW
	Efficiency	50	%
	Capital cost	3000	$/unit
	O&M cost	175	$/unit-year
	Replacement cost	2500	$/unit
	Lifespan	5	Year

The stored hydrogen energy in the HT (HT$_E$ (t)) and the stored hydrogen mass (HT$_m$ (t)) at time step (t) are expressed as follows (Sultan et al., 2021; Baghaee et al., 2016; Vendoti et al., 2021):

$$HT_E(t) = HT_E(t-1) + \left(P_{ELE/HT}(t) - \frac{P_{HT/FC}(t)}{\eta_{HT}} \right) \times \Delta t, \qquad (11)$$

$$HT_m(t) = HT_E(t) / HHV_H, \qquad (12)$$

Where $P_{HT/FC}(t)$ indicates the power supplied towards the FC from the HT, η_{HT} is the HT efficiency, Δt is the time durations during simulation, and HHV$_H$ denotes the higher heat value of the stored hydrogen gas (kWh/kg).

2.5. Fuel cell (FC) modeling

Fuel cells are electrochemical cells used to produce electrical energy through an electrochemical reaction by continuously supplying oxygen and hydrogen gases to the cell. At the anode, hydrogen is oxidized into protons (which rotate by the electrolyte to the anode) and electrons (which rotate from outside the cell to the anode), and after oxygen is collected, it is reduced to form water. Fuel cells produce electricity while having as byproducts

not only water, but also thermal energy (heat) (Wang et al., 2020, 2011). There are many types of fuel cells, the common types of fuel cells are Proton exchange membrane fuel cell, Alkaline fuel cells, Direct alcohol fuel cell, Molten carbonate fuel cell and Solid oxide fuel cell (Abdelkareem et al., 2021). In this study, a polymer electrolyte membrane (PEMFC) is used. PEMFC is characterized by its small size, long lifespan, and operation under relatively low temperatures (Samy and Barakat, 2020). The generated electrical power from PEMFC (FC$_P$) depends on its overall efficiency (η_{FC}) and can be expressed by Baghaee et al. (2016), Vendoti et al. (2021):

$$FC_P = \eta_{FC} * P_{HT/FC}, \qquad (13)$$

2.6. Converter unit

It is a power electronic device used for converting DC power from PV modules and FC into AC power to serve the loads. For the case study, the efficiency of the inverter (η_{inv}) used is 95%, and its lifespan is 15 years.

The generated power from renewable sources (P$_{ren}$) is expressed according to the following equation:

$$P_{ren}(t) = PV_P(t) + {BG_P(t)}/{\eta_{inv}}, \qquad (14)$$

3. Formulation of the optimization problem

3.1. Economic and cost analysis

The major goal of this section is to optimize the proposed isolated hybrid system to achieve a guaranteed supply of power at the lowest possible cost, which explains how to evaluate the total annual cost, the EC, and the net present cost (NPC). The present value of the principal investment and operating expenses over the project's lifetime is depicted by the NPC as (Das et al., 2019):

$$NPC = TAC/CRF, \tag{15}$$

Where TAC denotes the total annualized cost, which is the sum of the annualized cost of each subsystem component (C_A^y), and the capital recovery factor (CRF) is a conversion factor that is used to transform the initial principal cost into the annual capital cost. The CRF and C_{TA} are expressed as (Sultan et al., 2021):

$$CRF(R, S) = \frac{R(R + 1)^S}{(R + 1)^S - 1}, \tag{16}$$

$$TAC = \sum C_A^y = C_A^{PV} + C_A^{BG} + C_A^{ELE} + C_A^{HT} + C_A^{FC} + C_A^{inv}, \tag{17}$$

Where R is the interest rate, and S represents the lifespan of the proposed hybrid system. y denotes the subsystem components of the hybrid energy system, which are PV, biomass gasifier, electrolyzer, HT, FC, and power inverter. The C_A^y of each component is composed of annual capital cost ($C_{A\_Cap}^y$) of the system, annual replacement cost ($C_{A\_Rep}^y$) of the system, annual fuel cost (C_{A_fuel}) of BG, and annual operation and maintenance cost (C_{OM}^y) of the system, it can be expressed as (Das et al., 2019):

$$C_A^y = C_{OM}^y + C_{A\_Rep}^y + C_{A\_fuel} + C_{A\_Cap}^y, \tag{18}$$

$C_{A\_Cap}^y$ is the annualized capital cost for each unit which is the expenses that are spent for each component in the first year of the project's lifetime in order to make the system operational, it can be given by (Suresh and Meenakumari, 2019):

$$C_{A\_Cap}^y = CRF*C_{I\_Cap}^y, \tag{19}$$

$C_{I\_Cap}^y$ is the initial capital cost of the hybrid system.

The energy production cost (EC) ($/kWh) is the cost of one kWh produced from the hybrid system, and it is calculated as follows (Sultan et al., 2021):

$$EC(\$/kWh) = \frac{NPC (\$) * CRF}{\sum_1^{8760} Load_P(kWh)}, \tag{20}$$

Where $Load_P$ is the load power in (kWh).

3.2. Objective function

This work aims to establish an optimal combination of the system components to attain the maximum energy supply of the hybrid renewable energy system. This goal is achieved by minimizing the EC, maintaining high reliability of the power supply, minimizing the loss of power supply probability (LPSP) based on (22), and reducing the excess energy (P_{EXC}) absorbed by the dummy load (P_{Dum}) as to keep the overall system cost down. The P_{EXC} is defined by (23). The following expressions are used to calculate the values of the objective functions:

$$Min_X(F) = Min(\beta_1 EC + \beta_2 LPSP + \beta_3 P_{EXC}), \tag{21}$$

$$LPSP = \sum_1^{8760} \left(\frac{Load_P (t) - P_{ren} (t) - FC_P(t)}{Load_P(t)} \right) \tag{22}$$

$$P_{EXC} = \sum_1^{8760} (P_{Dum}/Load_P), \tag{23}$$

where β denotes the weight factor value of each objective function, and X represents the control variables of the optimization problem that must be optimized using the studied optimization algorithms, as given in the following formula:

$$X = [PV_N G_N HT_m P_{ELE/HT} FC_P], \tag{24}$$

3.3. Constraints

The optimization algorithm is working according to the following constraints and based on the upper and lower limits of the decision variables;

$$1 \leq \begin{bmatrix} PV_N \\ G_N \\ P_{ELE/HT} \\ FC_P \\ HT_m \end{bmatrix} \leq \begin{bmatrix} PV_N^{max} \\ G_N^{max} \\ P_{ELE/HT}^{max} \\ FC_P^{max} \\ HT_m^{max} \end{bmatrix}, \tag{25}$$

$$P_{EXC} \leq P_{EXE}^{max}, \tag{26}$$

$$LSPS \leq 0.06, \tag{27}$$

PV_N and G_N are set as integer numbers. PV_N^{max} and G_N^{max} are the maximum number of PV modules and gasifier generators, respectively. $P_{ELE/HT}^{max}$ and FC_P^{max} are the maximum rating in kW of the electrolyzer unit and the FC, respectively. HT_m^{max} denotes the maximum capacity of the HT in kg. P_{EXE}^{max} represents the maximum rating of the excess energy.

3.4. Operation strategy

The operation strategy used in the proposed hybrid system is simplified in a flowchart shown in Fig. 4. The operating strategy can be summarized in three main cases as follows:

When the energy produced from the renewable sources satisfies the load demand ($P_{ren} (t) = \frac{Load_P(t)}{\eta_{inv}}$), in this case, the generated power is supplied to cover the required load demand, and no power is needed from the FC, and no power is supplied to the electrolyzer;

When the energy produced from renewable sources exceeds the load demand ($P_{ren} (t) > \frac{Load_P(t)}{\eta_{inv}}$, in this case, this excess energy P_{EXC} (t) will feed the electrolyzer, and the produced hydrogen is used to charge the HT units;

When the energy produced from renewable sources is insufficient to meet the load demand ($P_{ren} (t) < \frac{Load_P(t)}{\eta_{inv}}$), in this case, the FC will use hydrogen stored in the HT units to make up for the deficiency in power generation. When the HT capacity reaches its minimum, this leads to load loss.

Each optimization technique used in this study works by following the steps below:

(1) Run the software of creating the proposed hybrid power system, and this step contains the following stages:

    (a) Generation of the initial population.
    (b) Run the code for creating the hybrid system, which is shown in the flowchart in Fig. 4, and stated in Eqs. (1) through (20).
    (c) The fitness functions are evaluated for all agents/ positions according to Eq. (21).

(2) Run the optimization technique with the proposed hybrid system, which includes the following stages:

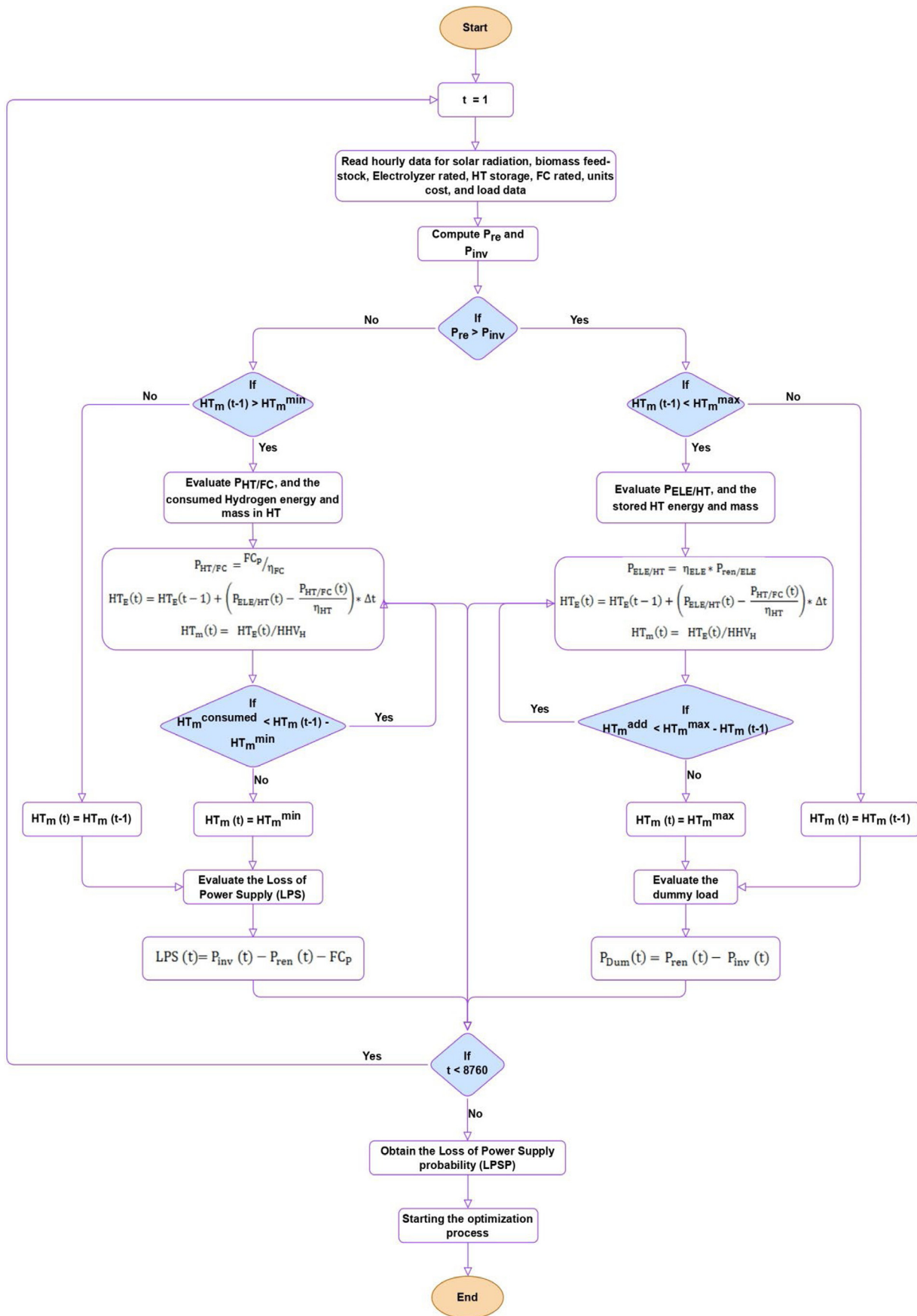   (a) Depending on the nature of each optimization technique used, the size of the system parts is updated.

Fig. 4. The flowchart of the operation strategy of the proposed hybrid system.

(b) Run the code for creating the hybrid system, which is shown in the flowchart in Fig. 4, and stated in Eqs. (1) through (20).

(c) The fitness functions are evaluated for all agents/positions according to Eq. (21).

(d) Examine whether the proposed system satisfies the end criterion or not. If so, (Yes), the code will be paused and will move to the following step; otherwise (No), the three previous stages from "a" to "c", will be repeated.

(e) Display the required results, including hybrid system sizing and EC, NPC, LPSP, and dummy load optimal values.

4. Proposed algorithms

4.1. The mayfly optimization algorithm (MOA)

Mayflies are a species of insects that belong to the order Ephemeroptera that originated from the so old group named Palaeoptera. The MOA algorithm can be called a modification of the standard PSO (Zervoudakis and Tsafarakis, 2020; Gao et al., 2020). The proposed MOA method combines the merits of the PSO, genetic algorithm (GA), and Firefly algorithm (FFA). The MOA is inspired by the patterns of the mating process of the mayflies. In the MOA, the males and females are arranged in different groups. In addition, the male mayflies are considered stronger than the female individuals, and then the males will do better in the optimization process. A group of males and another female group are randomly initiated. Each mayfly is considered a candidate solution in the search space of the optimization problem. The position of each individual determines the possibility of obtaining the desired optimal solution. The random location of the individuals in the search space is presented by the position vector $p = (p_1, p_2, \ldots\ldots, p_d)$, the performance of each mayfly is assessed regarding a certain objective function represented by f(x). The social and movement experiences of each individual in the search space determine the new path of the mayfly after updating its position using the velocity vector $v = (v_1, v_1, \ldots\ldots, v_d,)$. Each individual in the swarm decides its direction regarding its best position (pbest), while the best position obtained in the swarm by any individual is the global best position (gbest).

4.1.1. Movement of males

Similar to the PSO, the individuals in the swarm update their current position according to the following equation in which the position of certain mayfly i, in the current iteration (t) ($p_i(t)$) is updated by adding its velocity in the next iteration $v_i(t+1)$ (Gao et al., 2020),

$$p_i(t + 1) = p_i(t) + v_i(t + 1),\tag{28}$$

The male mayflies continue their nuptial dance up to some meters above the water level, and their velocity is updated as follows (Zervoudakis and Tsafarakis, 2020),

$$v_{ij}(t+1) = v_{ij}(t) + k_1 * e^{-\lambda r_p^2}(\text{pbest}_{ij} - p_{ij}(t)) + k_2 * e^{-\lambda r_g^2}(\text{gbest}_j - P_{ij}(t)),\tag{29}$$

Where k_1 and k_2 are attraction constants for evaluating the cognitive and social behaviors, respectively. λ is used to limit the visibility between individual mayflies. r_p and r_g denote the distance between the position of the individual in the current iteration $p_i(t)$ and its best position (pbest) and the global best position (gbest), respectively. The values of r_p and r_g are calculated according to Eqs. (30) and (31), respectively. v_{ij} and p_{ij} are the velocity and the location of the *i*th search agent in the *j*th dimension.

pbest_{ij} denotes the best position reached by the *i*th mayfly in the *i*th dimension. The best position of the *i*th search agent is determined according to the following formula,

$$\text{pbest}_i = \begin{cases} p_i(t + 1), f(p_i(t + 1)) < f(\text{pbest}_i) \\ \text{pbest}_i, \text{ otherwise} \end{cases},\tag{30}$$

Where f(.) is the objective function of the optimization problem. r_p and r_g are evaluated as follows,

$$r_p^2 = \left(\sum_{j=1}^{d}(p_{ij} - \text{pbest}_i)\right)^{1/2},\tag{31}$$

$$r_g^2 = \left(\sum_{j=1}^{d}(p_{ij} - \text{gbest}_i)\right)^{1/2}\tag{32}$$

To ensure the optimization algorithm's best performance, the best candidates should continue their up and down dancing. Therefore, the velocity of the best mayflies should continue to change. The velocity, in this case, is expressed as follows,

$$v_{ij}(t + 1) = v_{ij}(t) + c * \varepsilon,\tag{33}$$

Where ε is a random number in the range of $[-1, 1]$ and c is a coefficient describing the nuptial dancing of the mayflies.

4.1.2. Movement of females

The female mayflies do not fly in swarms like males. For the mating process, female mayflies move towards the location of the males. The position of a certain individual female mayfly in the search area $q_i(t)$ is updated as presented in the following equation (Zervoudakis and Tsafarakis, 2020; Gao et al., 2020),

$$q_i(t + 1) = q_i(t) + v_i(t + 1)\tag{34}$$

The authors of the MOA decided to model the attraction between males' and females' mayflies in a deterministic manner. The fittest female is proposed to be attracted to the fittest male, the second female towards the second male, etc. Consequently, the velocity of the female mayflies is determined using the following equation (Guo et al., 2021),

$$v_{ij}(t + 1) = \begin{cases} v_i(t) + k_2 * e^{-\eta r_{fm}^2}(p_{ij}(t) - q_{ij}(t)), f(q_i) > f(p_i) \\ u_{ij}(t) + c_\omega * \eta & f(q_i) \le f(p_i) \end{cases}\tag{35}$$

Where $q_{ij}(t)$ denotes the location of the *i*th female in the *j*th dimension during the iteration t. $u_{ij}(t)$ presents the velocity of the *i*th female mayfly in the *j*th dimension. r_{fm} denotes the distance between the male and female mayflies, and c_ω is the walk coefficient that is randomly selected in the case when a female mayfly is not attracted by any male.

4.1.3. Mating process

The way for the selection of the parents is the same as that used for the attraction of females by males' mayflies. The selection might be random or according to a certain objective function. When the mating is based on an objective function, the best fittest female mates with the corresponding best fittest male, the second female in the chain mates with the second fittest male in the swarm, and so on. Finally, two offspring are generated according to the following equation (Zervoudakis and Tsafarakis, 2020; Guo et al., 2021),

$$\text{offspring}_1 = \rho * \text{male} + (1 - \rho) * \text{female},\tag{36}$$

$$\text{offspring}_2 = \rho * \text{female} + (1 - \rho) * \text{male},\tag{37}$$

Table 4
Pseudo-Code of the MOA (Duman and Güler, 2018).

---

objective function represented by f(x), x = (x₁, x₂, ... xₐ)ᵀ
Initialize the male and female population pᵢ and qᵢ
Compute solutions
Evaluate the global best (gbest)
Do While stopping criteria are not met
        Update solutions and velocities of males and females
        Compute solutions
        Rank the mayflies
        Mate the mayflies
        Calculate offspring
        Separate offspring to male and female randomly
        Replace the worst solutions with the best new ones
        Update gbest and pbest
end while
Return
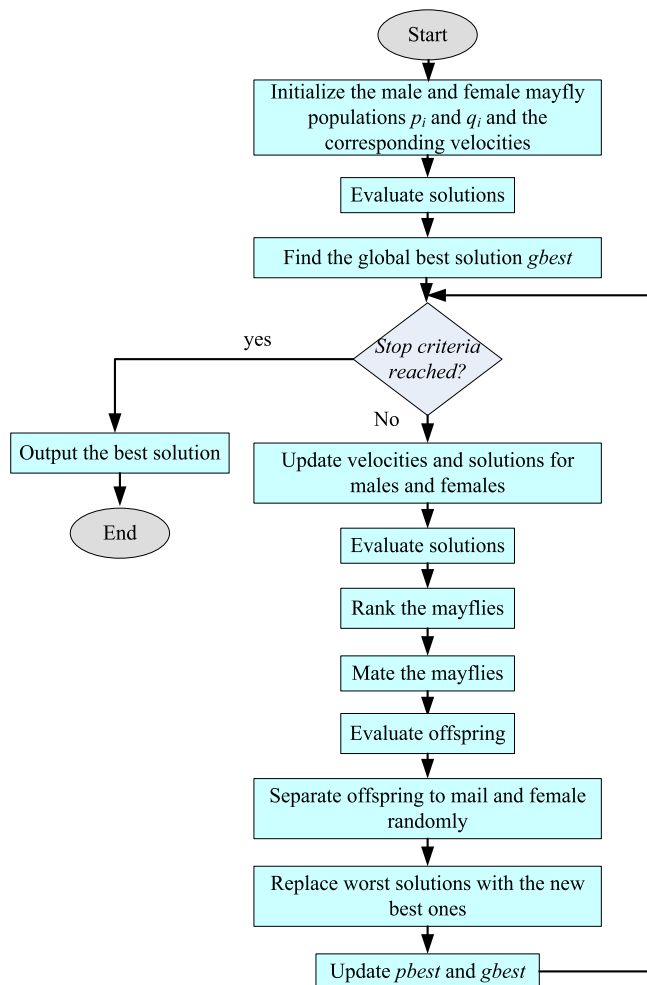
Fig. 5. Flowchart of the MOA method.

Where ρ is random numbers in Gauss distribution, the flowchart describing the procedure of the proposed MOA algorithm is shown in Fig. 5, while the block diagram of MOA used for optimizing the proposed hybrid renewable system is illustrated in Fig. 6, and the algorithm pseudo-code is presented in Table 4.

4.2. The Sooty Tern Optimization Algorithm (STOA)

STOA is a bio-inspired algorithm that has been validated using 44 benchmark test functions (Dhiman and Kaur, 2019). The re-

sults showed that STOA outperforms nine well-known optimization techniques in terms of performance. In addition, the results of the unimodal and multimodal test functions demonstrate the STOA algorithm's exploration and exploitation potencies. On the other hand, the results of CEC 2005 and CEC 2015 standard test functions prove that the STOA is capable of addressing high and challenging dimensionality bound-constrained actual situations. Statistical analysis has been carried out to establish the statistical significance of the STOA over benchmark test functions. Furthermore, to verify and demonstrate the performance of STOA on a given search space, it has been applied in 6 classic engineering structure problems, namely; pressure vessel design, speed reducer design, welded beam design, tension/compression spring design, 25-bar truss design, and rolling element bearing design problems (Dhiman and Kaur, 2019).

However, sooty terns are species of birds that are found in all regions of the world and are scientifically called Onychoprion fuscatus. STOA stimulates the attacking and migration behavior of sooty tern birds in nature. Sooty terns generally live in colonies, and they use their natural intelligence in attacking their prey (Dhiman and Kaur, 2019). The following features characterize the migration behavior of the sooty terns:

- During seasonal movements, sooty terns fly in groups while their initial position within the same group is different to prevent collisions in the group,
- In the same group, all individuals can fly in the direction of the fittest sooty tern,
- All individuals in a particular group update their location regarding the best fittest candidate,
- During movement in the air, sooty terns use the spiral-shaped mechanism surrounding the prey and attacking it.

During the migration stage, the sooty terns should satisfy some conditions such as avoidance of collision, flying, and converging towards the best sooty tern in the group, updating location according to the location of the best fittest sooty tern. The mathematical representation of the migration behavior is given in Eqs. (37) to (41) (Dhiman and Kaur, 2019).

$$C_i = D_A * X_i(it), \tag{38}$$

$$D_A = C_f - (it * {}^{C_f/Max_{it}}), \tag{39}$$

Where C_i denotes the location of the search agent, X_i (it) denotes the current location of the sooty tern at the it-th iteration, D_A presents the movement of the sooty tern (search agent) in the search field, C_f is a controlling coefficient that decreases from C_f to zero and used for adjusting the movement in the search field, and Max_{it} denotes the maximum iteration number.

$$R_i = C_B * (X_{best}(it) - X_i(it)), \tag{40}$$

$$C_B = 0.05 * rand(0, 1), \tag{41}$$

Where R_i denotes the various positions of the search agent X_i (it) in the search space in its movement towards the best fittest sooty tern, C_B denotes a uniformly distributed arbitrary coefficient.

$$G_i = C_i * R_i, \tag{42}$$

Where G_i denotes the distance between the search agent and the best one.

During migration time, sooty terns have the ability to change the speed and the direction of the attack. During the attack, sooty terns move towards the prey in a spiral shape that can be presented by the following equations (Dhiman and Kaur, 2019),

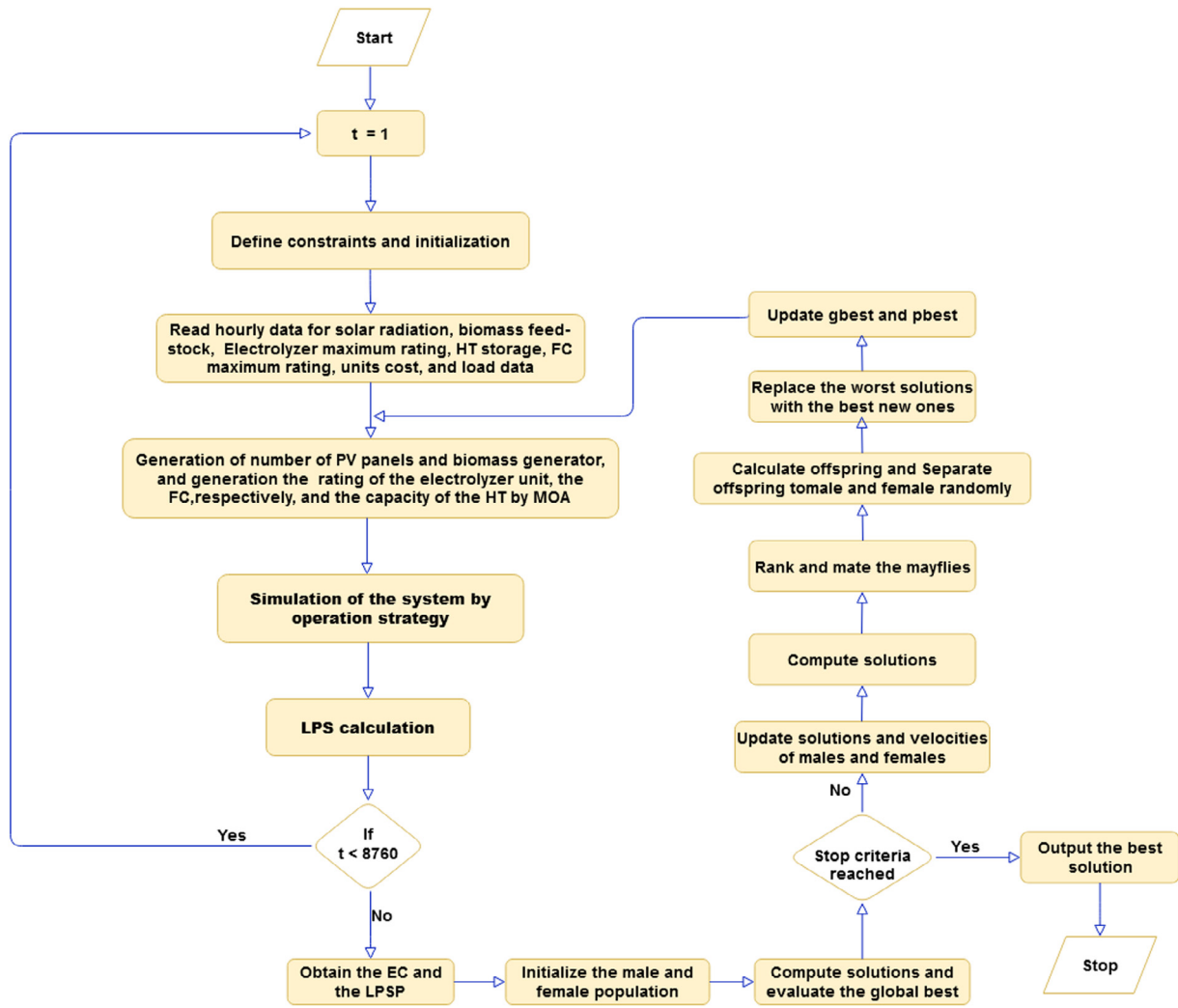$$x' = Radius * sin(m), \tag{43}$$

$$y' = Radius * cos(m), \tag{44}$$

Fig. 6. Block diagram of MOA used for optimizing the proposed hybrid systems.

$$z' = \text{Radius} * m, \tag{45}$$

$$R = u * e^{kv}, \tag{46}$$

Where x', y', and z', denote the angle of attack; Radius denotes the radius of each turn in the spiral; m is a variable that ranges between ($0 \leq k \leq 2\pi$); u and v are factors describing the spiral shape. The updated position of the candidate search agent is computed according to the following equation,

$$X_i(t) = (R_i(it) * (x' + y' + z')) * X_{\text{best}}(it), \tag{47}$$

The flowchart of the proposed STOA algorithm is shown in Fig. 7, while the block diagram of STOA used for optimizing the proposed hybrid renewable system is illustrated in Fig. 8 and the algorithm pseudo-code is presented in Table 5.

4.3. The Whale Optimization Algorithm (WOA)

The Whale Optimization Algorithm (WOA) has been proposed by Mirjalili et al. (Mirjalili and Lewis, 2016). WOA is a recent heuristic optimization method; it is based on imitating the whale's social behavior and is inspired by the humpback whale's bubble-net hunting behavior. The WOA technique starts with a set of random individuals. Individuals update their places in relation to either a randomly chosen search agent or the best solution

obtained at each iteration. There is a variable called A, which is a control variable that is varied from 2 to 0 to allow exploration and exploitation, respectively. When $|A| > 1$, a random search agent is picked, while in case $|A| < 1$, the best solution is chosen for updating the search agents' positions. To balance the exploration/exploitation capabilities, WOA can switch between a spiral and a circular movement based on the value of another variable called p. The pseudo-code of the WOA technique is indicated in Table 6.

4.4. The Sine cosine optimization algorithm (SCA)

A meta-heuristic optimization method called sine cosine algorithm (SCA) has been created by Mirjalili et al. (Mirjalili, 2016). The SCA optimization method includes the transportation of population members within the search space, presenting an approach to the issue. SCA uses trigonometric sine and cosine formulas for this purpose. SCA begins by producing a set of random solutions. These solutions are iterated during the optimization process to improve them. At each step of the calculation, solutions are updated based on the next formulas;

$$X_i^{it+1} = \begin{cases} X_i^{it} + r_1 \sin(r_2) \left| r_3 P_i^{it} - X_i^{it} \right|, r_4 < 0.5 \\ X_i^{it} + r_1 \cos(r_2) \left| r_3 P_i^{it} - X_i^{it} \right|, r_4 \geq 0.5 \end{cases}, \tag{48}$$

Table 5

Pseudo-Code of the STOA (Dhiman and Kaur, 2019).

Initialize the population $X_i^p = (X_1^p, X_2^p, X_3^p, \ldots \ldots, X_N^p)$ within the limits $X_i^{min} \leq X_i^p \leq X_i^{max}$
Initialize parameters D_A and C_B
Evaluate the fitness of the whole population
Best search agent $\rightarrow X_{best}$
While (it < Max$_{it}$)
    for (i = 1: N)
    Update the position of the current search agent
    end for
    Initialize parameters D_A and C_B
    Evaluate the fitness of the whole population
    Update X_{best}
    it = it +1
end while
Return

Table 6

Pseudo-Code of the WOA (Mirjalili and Lewis, 2016).

Initialize the population $X_i^p = (X_1^p, X_2^p, X_3^p, \ldots \ldots, X_N^p)$ within the limits $X_i^{min} \leq X_i^p \leq X_i^{max}$

Evaluate the fitness of each search agent
Best search agent $\rightarrow X_{best}$
While (it < Max$_{it}$)
    for each search agent
    Update a, A, C, l and p
        if1 ($p < 0.5$)
          if2 (|A| <1)
             Update the position of the current search agent
         else if2 (|A| ≥1)
             Select a random search agent (X_{rand})
              Update the position of the current search agent
        end if2
        else if1 (p ≥0.5)
             Update the position of the current search agent
        end if1
    end for
    Check if any search agent goes beyond the search space and amend it
    Evaluate the fitness of each search agent
    Update X_{best} if there is a better solution
    it = it +1
end while
return X_{best}

Table 7

Pseudo-Code of the SCA (Mirjalili, 2016).

Start the population of the solution
Initialize r_1, r_2, r_3, and r_4 values
Do
    Compute the objective function for each solution
    Evaluate the best solution
While (it < Max$_{it}$)
    Update r_1, r_2, r_3, and r_4 values
    Update the obtained solution
end while
Return the best solution

Where X_i^{it} is the current individual (i) at iteration (it), P_i^{it} denotes the best individual's position, and r_1, r_2, r_3, and r_4 are the four random control parameters used to prevent becoming stuck in poor solutions and keep the exploration and exploitation processes in balance. The pseudo-code of the SCA technique is indicated in Table 7.

5. Results and discussion

5.1. Meteorology of the case study area

Abu-Monqar is a remote Egyptian settlement in the Western Desert of Egypt. It is a remote oasis located 100 km south of Frafra Oasis, 250 km from the El- Dakhla Oasis, and 650 km southwest of Cairo. The selected area's latitude and longitude are 26°30.3′ North and 27°39.8′ East, respectively (Diab et al., 2019). The system average load value used for simulation is 260 kW, and the peak value is 420 kW (Diab et al., 2019). Fig. 9 shows the hourly load power over one summer day and one year (Diab et al., 2019). The monthly average global solar radiation and temperature for one year are taken from the SOLAR RADIATION AND METEOROLOGICAL DATA SERVICES (Anon, 2021c), which is based on the average long-term values over 20 years from the NASA Surface Meteorology and Solar Energy website for the proposed case study area. The hourly average solar radiation on the horizontal plane and temperature during one year and a summer day are shown in Figs. 10 and 11, respectively.

Biomass energy is one of the renewable energies that can be found almost anywhere because it is formed from organic materials, either directly from plants or indirectly from industrial, agricultural, and household products (El-Sattar et al., 2020a). Biomass energy can be converted as a source of electricity or heat using several technologies such as thermolysis, anaerobic digestion, and gasification (Bakheet et al., 2018). Egypt is one of the agricultural countries, which means the availability of agricultural residues that can be used as biomass feedstock. Rice straw is one of the feed stocks with the greatest potential for energy production, which is abundant in the north, corn stalk in the middle of Egypt, and sugar cane in the south (Food and Agriculture Organization of the United Nations, 2017). In this study, corn stalk is used due to its availability in areas near the study area. The amount of feedstock used during each month is shown in Fig. 12.
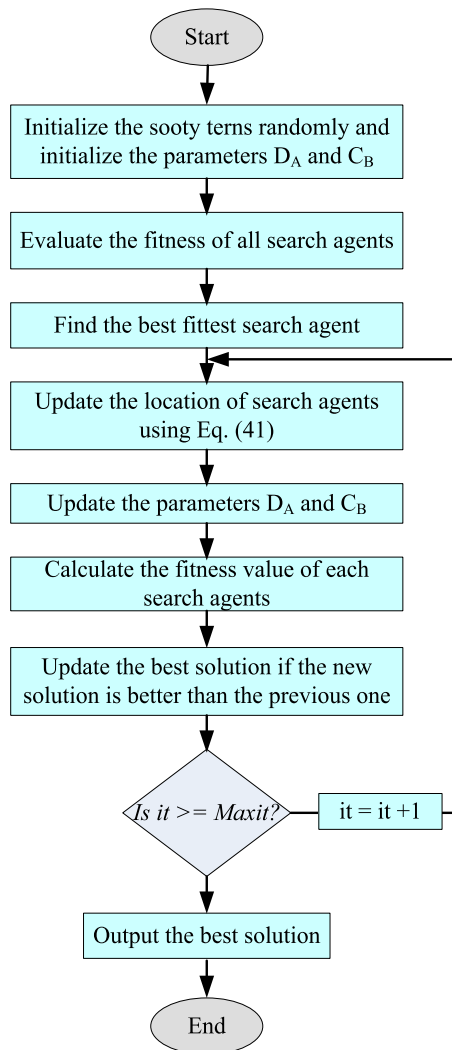
Fig. 7. Flowchart of the STOA method.

5.2. Discussion of the optimal results

A new application for a recent MOA is proposed in this work for designing the optimum sizing of stand-alone PV, BG, FC, Electrolyzer units, and HT systems. The proposed algorithm's results are compared with those obtained by other recent methods, STOA, WOA, and SCA, in order to affirm the proposed MOA's efficacy in achieving the highest reliability and lowest cost.

The studied optimization algorithms are coded and implemented using MATLAB software. For each optimization algorithm, 50 independent runs are conducted, and the results are recorded to compare the algorithms' accuracy. The parameters used in each algorithm are given as:

- MOA: Population Size (males and females) =20, Maximum number of iterations (Max_{it}) = 100, and dimension size = 5, Personal Learning Coefficient =1, Global Learning Coefficient =1.5. Distance sight Coefficient = 2, Damping Ratio = 0.8, Random flight = 1.
- STOA: Number of search agents (N_{search}) = 20, Max_{it} = 100, and dimension size = 5, a linearly decreased from 2 to 0.
- WOA: N_{search} = 20, Max_{it} = 100, dimension size = 5, a linearly decreased from 2 to 0.

- SCA: N_{search} = 20, Max_{it} = 100, dimension size = 5, a linearly decreased from 2 to 0.

Fig. 13 displays the convergence curves of the optimization process based on MOA, STOA, WOA, and SCA techniques. These optimization algorithms have been applied 50 runs for 100 iterations to assess the best fitness function value to subjugate the proposed algorithms' randomness and verify their stability and robustness. For the proposed case study, each optimizer is used in the same way. The final values of the proposed MOA's objective function are within a small range, demonstrating MOA's consistency in finding the best solution for the optimization problem.

Fig. 14 shows a comparison between the convergence curves for the best implementation within the 50 runs of the optimization programs for the different algorithms. According to the convergence characteristics, MOA has the best results in achieving the minimum fitness value after 44 iterations, outperforming STOA, WOA and SCA.

Table 8 indicates the results of the optimal sizing characteristics of the hybrid microgrid for the four optimization algorithms used in this study. These results include the best fitness function, the number of iterations to reach the optimal solution, the optimal values of the decision variables, EC ($/kWh), NPC ($), LPSP (%), and GHG (ton/y). This table shows that the MOA has the best fitness function with 0.1219998, followed by STOA, SCA, and WOA with 0.1221296, 0.1224865, and 0.1251143, respectively. By comparing the results provided in the table, it can be noticed that the MOA is characterized by the minimum EC, the minimum NPC, and the lowest GHG, compared with the rest of the used algorithms, followed by the STOA, SCA, and WOA. The values of the LPSP obtained from all algorithms are within constraints.

Fig. 15 shows the contribution of the annual cost of each unit (representing the operating and maintenance costs, which are costs spent each year) of the proposed hybrid system for the MOA algorithm. As is evident, the FC represents the highest annual percentage cost with 36% of the total cost of the proposed system, followed by PV modules with 19%, then the Electrolyzer units with 18%, inverter with 14%, biomass system with 11%, and finally the HT with 2%. The results from the MOA indicated that the annual percentage cost of the FC represents the largest portion of all units.

Fig. 16 reveals the contribution of each unit to the NPC percentage of the proposed hybrid system using the MOA. The results revealed that the NPC of the PV modules accounts for the largest portion with 27% (1,066,906 $), followed by the Electrolyzer unit with 25% (1,006,631$), the FC with 18% (728,728 $), the biomass system with 15% (614,001$), the inverter with 12% (488,132$), and the HT represents the lowest NPC value with 3% (134,966$).

Fig. 17 indicates the hybrid PV, BG, and FC power system's power output performance over a 24-hour cycle for four different days with high energy consumption over the year. According to the obtained results, the excess power from PV and BG units (P_{ren}) is used to power the electrolyzer for hydrogen production. When the power generated by the P_{ren} is not able to meet the load power needs, then the FC will use the hydrogen stored in the HT unit to make up for the shortage in power generation. Fig. 18 shows the variation in the stored mass amounts of hydrogen in each hour in the HT during one year (8760 h) in case of using the MOA method. It can be noticed that the maximum amount of hydrogen mass stored is 63 kg.

6. Conclusions

This work's main objective is to assist officials, decision-makers, and the private sector in identifying advantages, opportunities,
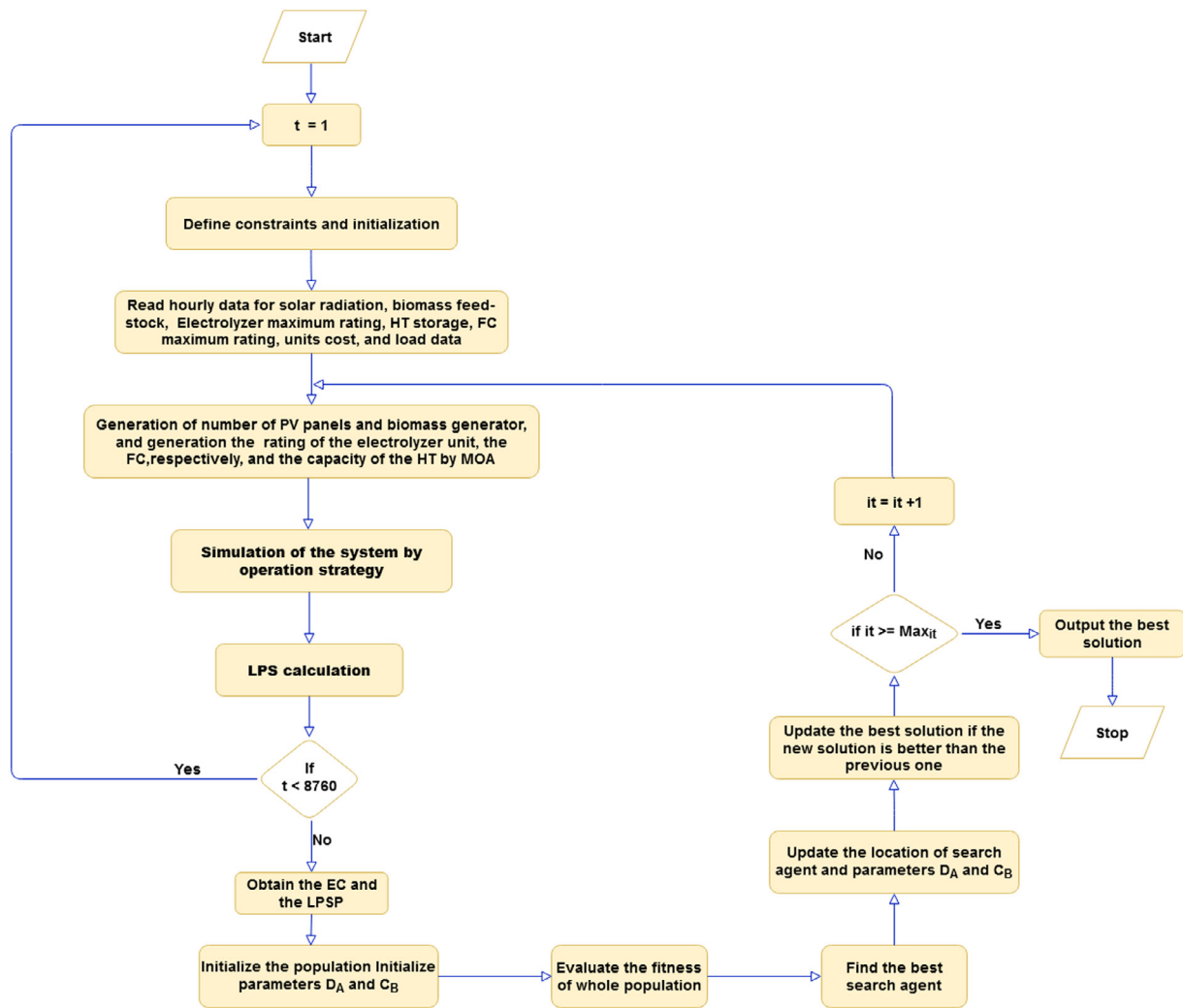
Fig. 8. Block diagram of STOA used for optimizing the proposed hybrid system.
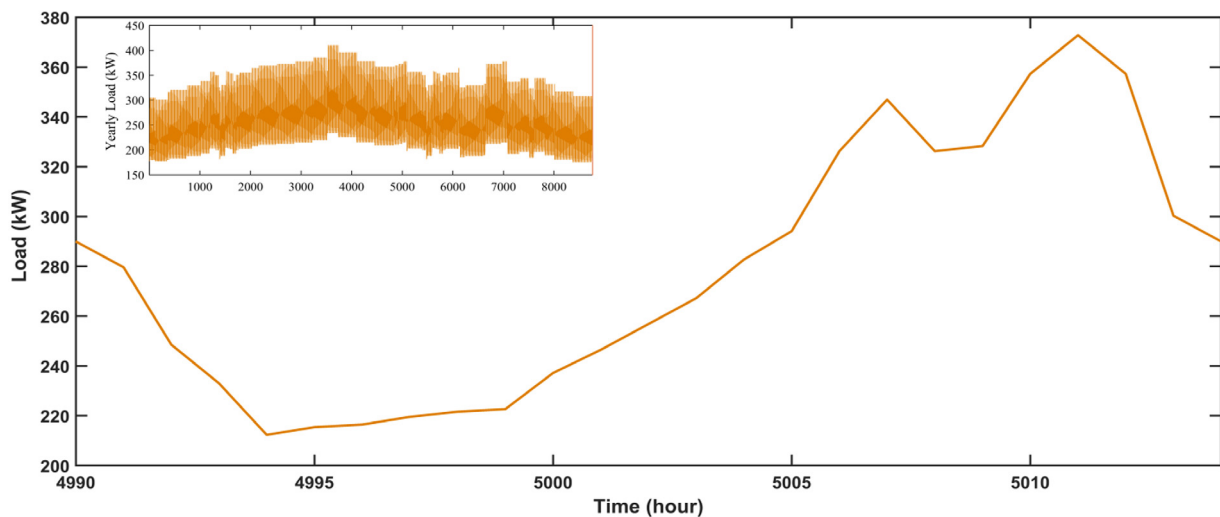

Fig. 9. Daily and yearly load profile.

and obstacles to the future of solar and biomass energy in Egypt and potential profit opportunities. Hence, this will attract investments by the private sector to expand the use of solar and biomass energy as an alternative to traditional energy.

In this paper, a recent optimization technique called MOA has been utilized to design a small stand-alone microgrid with the aim of meeting the electricity requirements of a small remote area in the Western Desert of Egypt with a peak load of 420 kW.
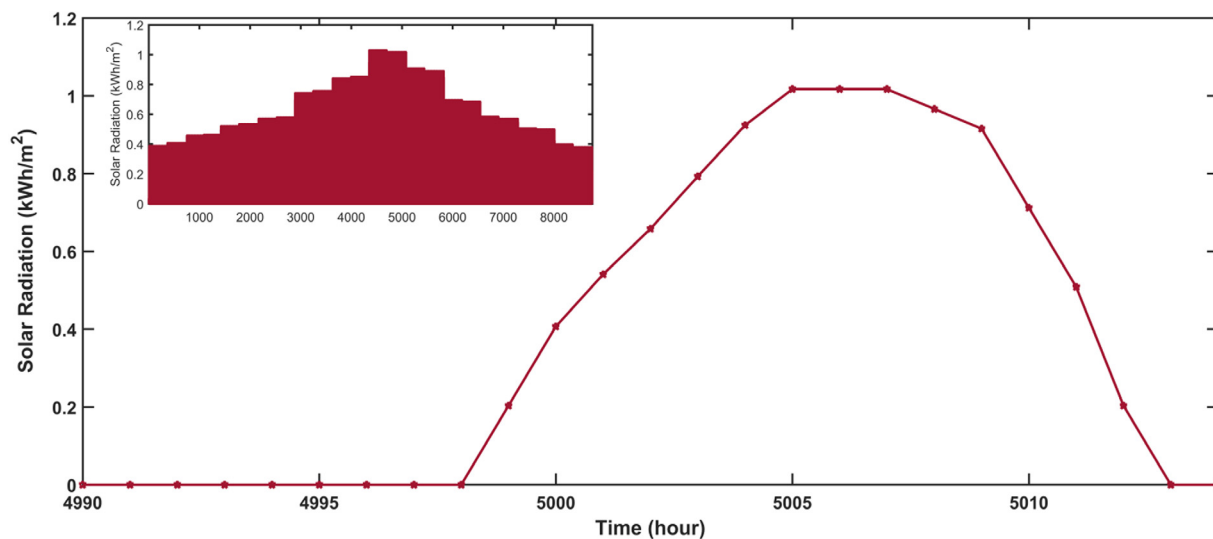
Fig. 10. Hourly PV average radiation during one year and a summer day.
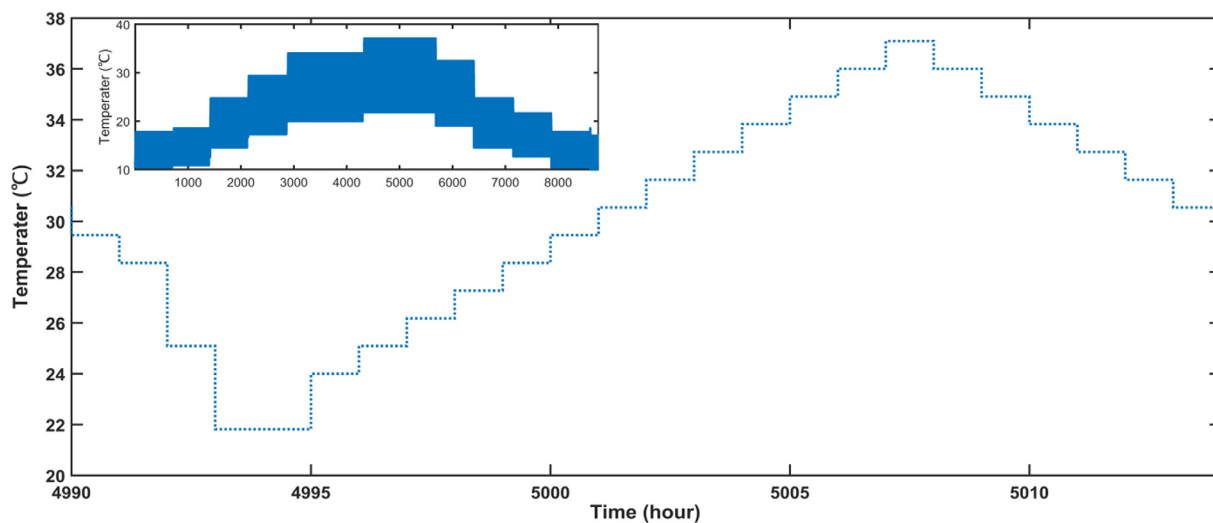
Fig. 11. Hourly PV average temperature during one year and a summer day.
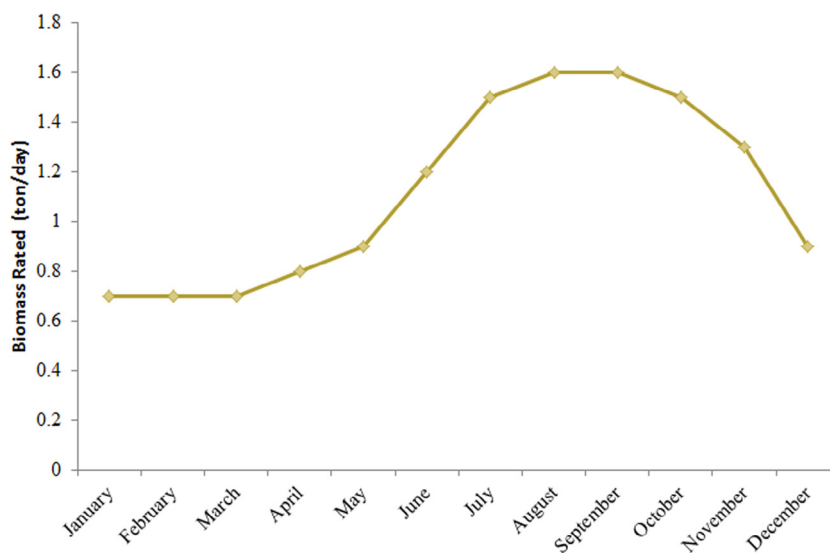
Fig. 12. The rate of the feedstock used during a year.
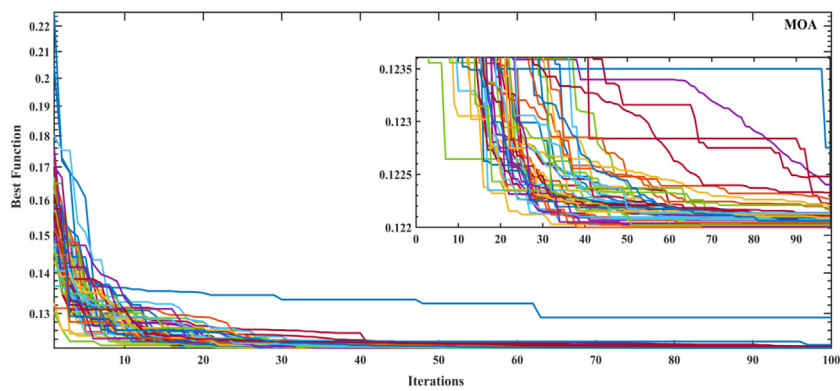
(a)
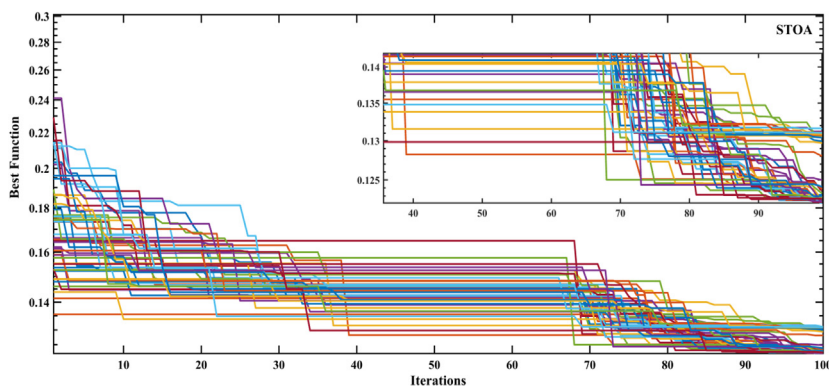
(b)
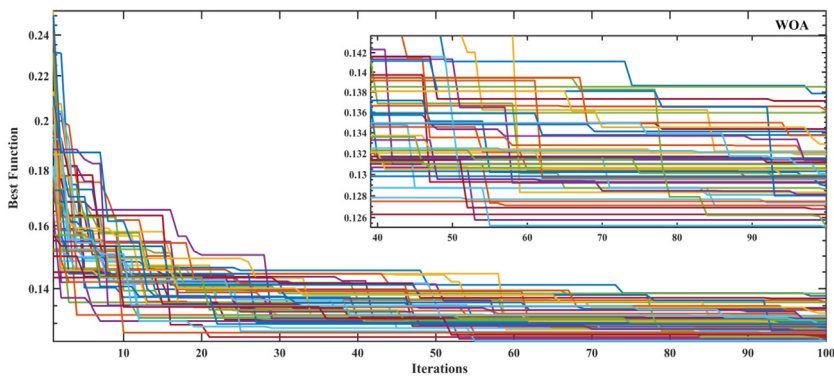
(c)
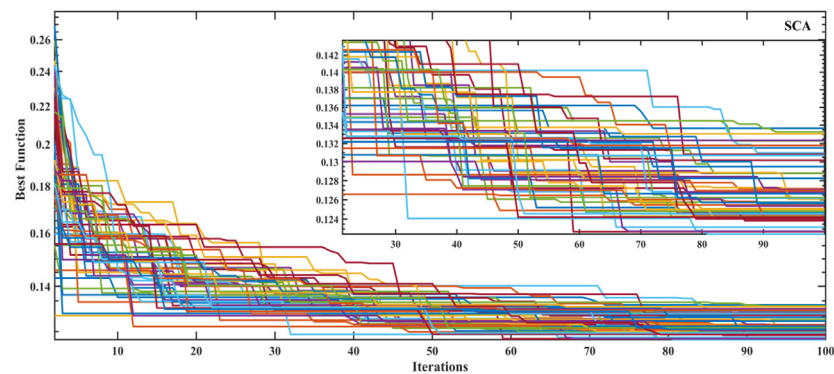
(d)

Fig. 13. The convergence curves of the studied algorithms for 100 iterations, (a) MAO, (b) STOA, (c) WOA, (d) SCA.

Table 8

The Optimization Features Parameters for the Proposed Hybrid System Based On Using MOA, STOA, WOA, and SCA.

	MOA	STOA	SCA	WOA
Best Fitness Function	**0.1219998**	0.1221296	0.1224865	0.1251143
Iteration Number	**44**	41	27	33
PV (units)	**47**	42	41	51
Nominal PV power (kW)	46.7	41.92	40.1	50.79
Generators (units)	**2**	3	3	3
Nominal generator power (kW)	72	84.9	86	89.6
Electrolyzer rated (kW)	319.87	326.35	323.419	336.78
Hydrogen tank (kg)	62.48	61.28	66.15	67.41
Fuel cell (kW)	124.71	130.09	134.927	155.03
EC ($/kWh)	**0.2106533**	0.210961	0.2123484	0.2367564
NPC ($)	**6,170,134**	6,179,148	6,219,783	6,934,705
LPSP (%)	**0.05993**	0.059411	0.059187	0.0365246
GHG (ton/y)	**792.534**	806.654	808.559	849.626
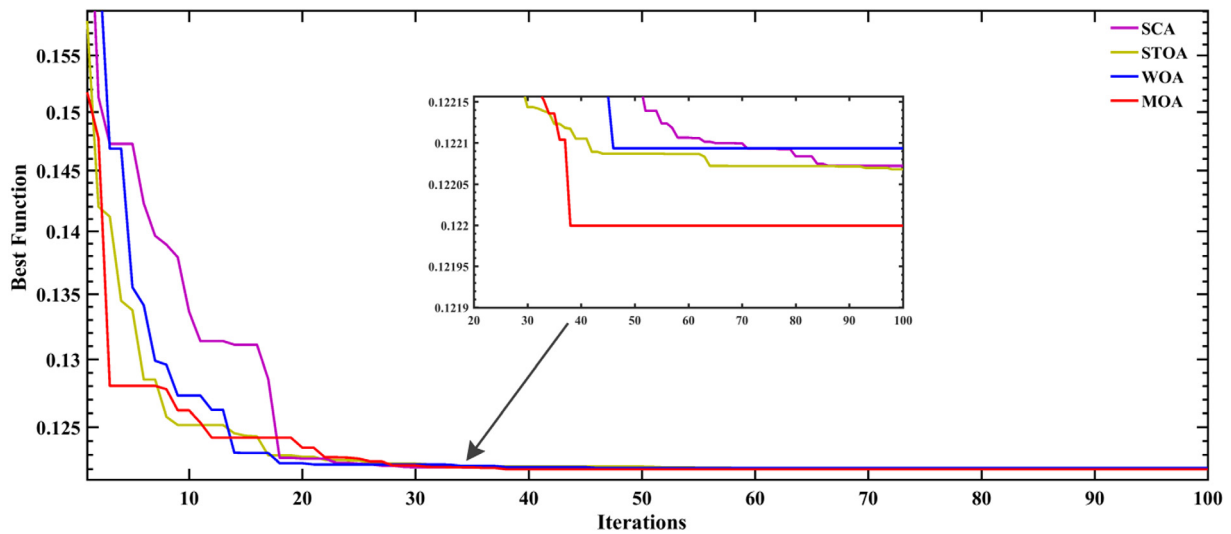
Fig. 14. The convergence curves for the best implements using MOA, STOA, WOA and SCA for 100 iterations.

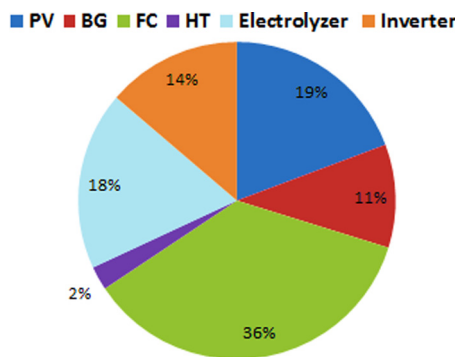**Fig. 15.** Break down of the annual costs of the hybrid system's units.
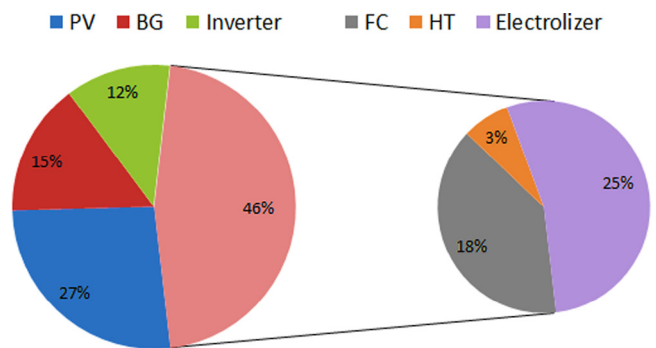

Fig. 16. Break down of the NPC of the hybrid system units using MOA.

This hybrid power system is based on two renewable resources, the PV modules and biomass generating system integrated with the FC and an electrolyzer for hydrogen production. This work aims to reduce the energy production cost, NPC, and GHG while maintaining high values of power supply reliability. In order to assess the accuracy of the proposed algorithm, its results have been compared with those obtained by other well-known techniques; STOA, WOA, and SCA. The simulation results demonstrated the proposed algorithm's effectiveness in identifying the optimal capacities of the generating and energy storage units in the proposed grid-independent hybrid system. The MOA has achieved the best optimal solution for the proposed system after 44 iterations with the minimum EC of 0.2106533 $/kWh, NPC of 6,170,134 $, LPSP of 0.05993%, and GHG of 792.534 t/y.
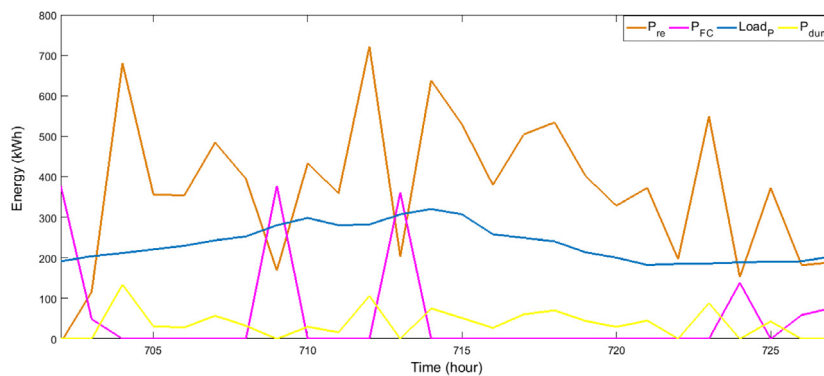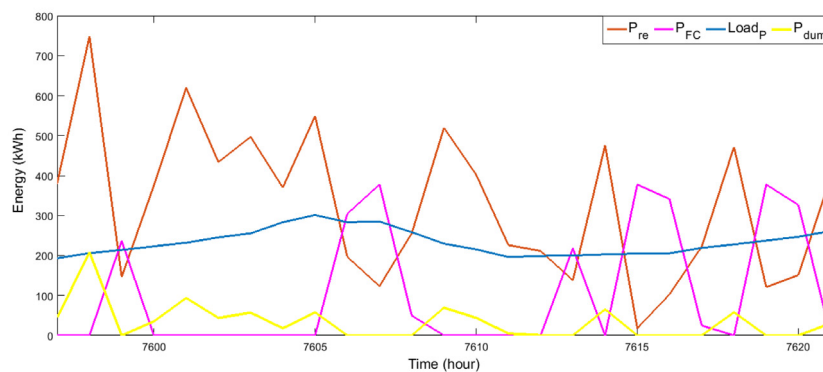
(a) a day of Winter season
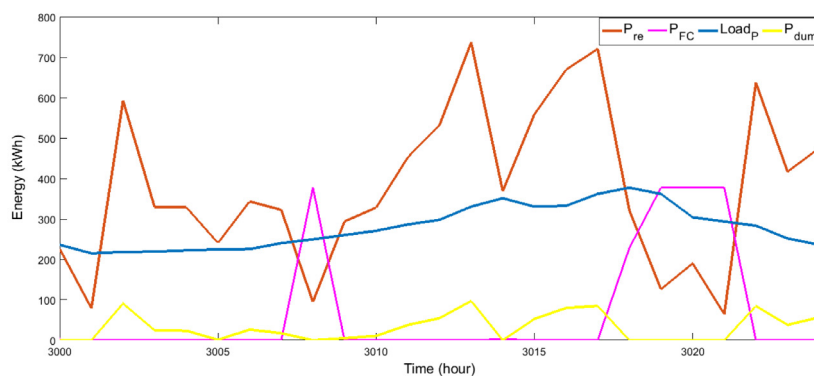
(b) a day of Spring season
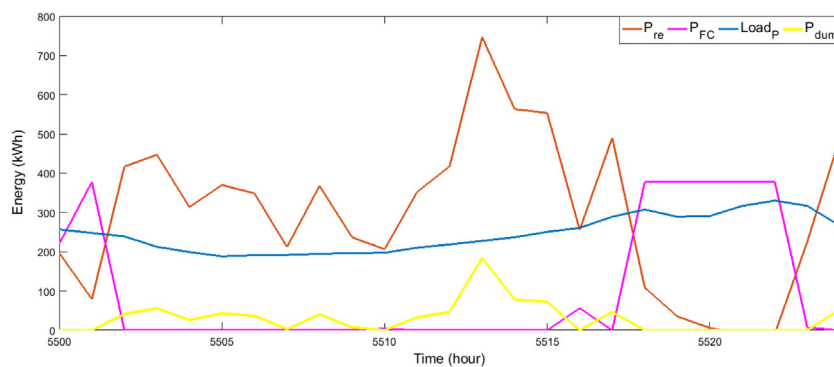
(c) a day of Summer season

(d) a day of Autumn season

Fig. 17. The operation capacity of the proposed hybrid system for 4 different days using MOA.
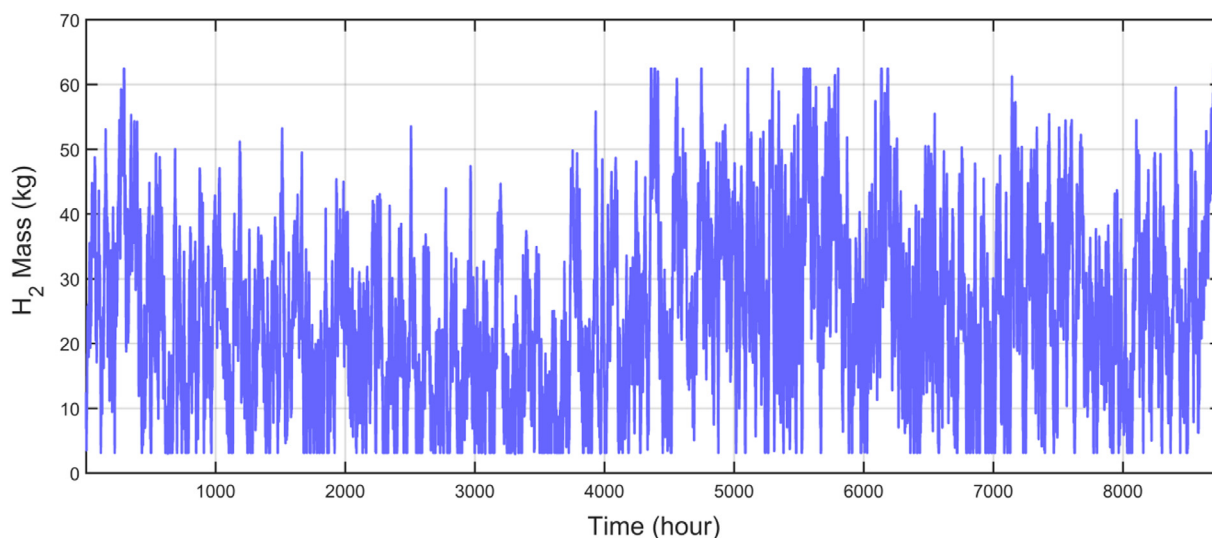
Fig. 18. The hourly change in the mass of hydrogen stored during a year.

Declaration of competing interest

The authors declare that they have no known competing financial interests or personal relationships that could have appeared to influence the work reported in this paper.

Data availability

Data will be made available on request.

References

Abdelhady, S., Shalaby, M.A., Shaban, A., 2021. Techno-economic analysis for the optimal design of a national network of agro-energy biomass power plants in Egypt. Energies 14, http://dx.doi.org/10.3390/en14113063.

Abdelkareem, M.A., Elsaid, K., Wilberforce, T., Kamil, M., Sayed, E.T., Olabi, A., 2021. Environmental aspects of fuel cells: A review. Sci. Total Environ. 752, 141803. http://dx.doi.org/10.1016/j.scitotenv.2020.141803.

Alshammari, N., Asumadu, J., 2020. Optimum unit sizing of hybrid renewable energy system utilizing harmony search, Jaya and particle swarm optimization algorithms. Sustain. Cities Soc. 60, 102255. http://dx.doi.org/10.1016/j.scs.2020.102255.

Alturki, F.A., Awwad, E.M., 2021. Sizing and cost minimization of standalone hybrid WT/PV/Biomass/Pump-Hydro storage-based energy systems. Energies 14, 489. http://dx.doi.org/10.3390/en14020489.

Anon, 2021a. Egypt - Renewable energy. Available online: https://www.trade.gov/knowledge-product/egypt-renewable-energy. (Accessed 7 February 2021).

Anon, 2021b. Egypt - Renewable energy | privacy shield. Available online: https://www.privacyshield.gov/article?id=Egypt-Renewable-Energy. (Accessed 7 February 2021).

Anon, 2021c. MERRA - SoDa. Available online: https://www.soda-pro.com/web-services/meteo-data/merra?fbclid=IwAR2vTObCUaC3DpZev3PqLX0FwV-XATjk0E2qDqp1ZRCWIcVxBQBv6eeWTUA. (Accessed 1 April 2022).

Anon, 2021d. The ministry of electricity and renewable energy. Available online: http://www.moee.gov.eg/english_new/home.aspx. (Accessed 7 February 2021).

Anon, 2021e. Renewable energy outlook: Egypt. Available online: https://www.irena.org/publications/{2018}/Oct/Renewable-Energy-Outlook-{Egypt}. (Accessed 7 February 2021).

Anon, 2021f. Renewables - fuels & technologies - IEA. Available online: https://www.iea.org/fuels-and-technologies/renewables. (Accessed 6 February 2021).

Anon, 2021g. World energy outlook 2020 – analysis - IEA. Available online: https://www.iea.org/reports/world-energy-outlook-2020. (Accessed 6 February 2021).

Anoune, K., Ghazi, M., Bouya, M., Laknizi, A., Ghazouani, M., Abdellah, A. Ben, Astito, A., 2020. Optimization and techno-economic analysis of photovoltaic-wind-battery based hybrid system. J. Energy Storage 32, 101878. http://dx.doi.org/10.1016/j.est.2020.101878.

Attemene, N.S., Agbli, K.S., Fofana, S., Hissel, D., 2020. Optimal sizing of a wind, fuel cell, electrolyzer, battery and supercapacitor system for off-grid applications. Int. J. Hydrogen Energy 45, 5512–5525. http://dx.doi.org/10.1016/j.ijhydene.2019.05.212.

Baghaee, H.R., Mirsalim, M., Gharehpetian, G.B., Talebi, H.A., 2016. Reliability/cost-based multi-objective Pareto optimal design of stand-alone wind/PV/FC generation microgrid system. Energy 115, 1022–1041. http://dx.doi.org/10.1016/j.energy.2016.09.007.

Bakheet, S., Kamel, S., El-Sattar, H.A., Jurado, 2018. Different biomass gasification reactors for energy applications. In: Proceedings of the 2018 Twentieth International Middle East Power Systems Conference. MEPCON, IEEE, pp. 660–665.

Bukar, A.L., Tan, C.W., Lau, K.Y., 2019. Optimal sizing of an autonomous photovoltaic/wind/battery/diesel generator microgrid using grasshopper optimization algorithm. Sol. Energy 188, 685–696. http://dx.doi.org/10.1016/j.solener.2019.06.050.

Cano, A., Arévalo, P., Jurado, F., 2020. Energy analysis and techno-economic assessment of a hybrid PV/HKT/bat system using biomass gasifier: Cuenca-Ecuador case study. Energy 202, 117727. http://dx.doi.org/10.1016/j.energy.2020.117727.

Chen, L., Xu, C., Song, H., Jermsittiparsert, K., 2021. Optimal sizing and sitting of EVCS in the distribution system using metaheuristics: A case study. Energy Rep. 7, 0–9. http://dx.doi.org/10.1016/j.egyr.2020.12.032.

Das, M., Singh, M.A.K., Biswas, A., 2019. Techno-economic optimization of an off-grid hybrid renewable energy system using metaheuristic optimization approaches – Case of a radio transmitter station in India. Energy Convers. Manag. 185, 339–352. http://dx.doi.org/10.1016/j.enconman.2019.01.107.

Dhiman, G., Kaur, A., 2019. STOA: A bio-inspired based optimization algorithm for industrial engineering problems. Eng. Appl. Artif. Intell. 82, 148–174. http://dx.doi.org/10.1016/j.engappai.2019.03.021.

Diab, A.A.Z., Sultan, H.M., Mohamed, I.S., Kuznetsov, O.N., Do, T.D., 2019. Application of different optimization algorithms for optimal sizing of PV/Wind/Diesel/Battery storage stand-alone hybrid microgrid. IEEE Access 7, 119223–119245. http://dx.doi.org/10.1109/access.2019.2936656.

Dong, W., Li, Y., Xiang, J., 2016. Optimal sizing of a stand-alone hybrid power system based on battery/hydrogen with an improved ant colony optimization. Energies 9, http://dx.doi.org/10.3390/en9100785.

Duman, A.C., Güler, Ö., 2018. Techno-economic analysis of off-grid PV/wind/fuel cell hybrid system combinations with a comparison of regularly and seasonally occupied households. Sustain. Cities Soc. 42, 107–126. http://dx.doi.org/10.1016/j.scs.2018.06.029.

El-Sattar, H.A., Kamel, S., Jurado, F., 2020a. Fixed bed gasification of corn stover biomass fuel: Egypt as a case study. Biofuels, Bioprod. Biorefining 14, 7–19. http://dx.doi.org/10.1002/bbb.2044.

El-Sattar, H.A., Kamel, S., Tawfik, M.A., Vera, D, 2016. Modeling of a downdraft gasifier combined with externally fired gas turbine using rice straw for generating electricity in Egypt. In: Proceedings of the 2016 Eighteenth International Middle East Power Systems Conference. MEPCON, IEEE, pp. 747–752.

El-Sattar, H.A., Kamel, S., Tawfik, M.A., Vera, D., Jurado, F., 2018. Modeling and simulation of corn stover gasifier and micro-turbine for power generation. Waste Biomass Valoriz. 10, 1–14. http://dx.doi.org/10.1007/s12649-018-0284-z.

El-Sattar, H.A., Kamel, S., Vera, D., Jurado, F., 2020b. Tri-generation biomass system based on externally fired gas turbine, organic rankine cycle and absorption chiller. J. Clean. Prod. 260. http://dx.doi.org/10.1016/j.jclepro.2020.121068.

Eteiba, M.B., Barakat, S., Samy, M.M., Wahba, W.I., 2018. Optimization of an off-grid PV/Biomass hybrid system with different battery technologies. Sustain. Cities Soc. 40, 713–727. http://dx.doi.org/10.1016/j.scs.2018.01.012.

Fathy, A., 2016. A reliable methodology based on mine blast optimization algorithm for optimal sizing of hybrid PV-wind-FC system for remote area in Egypt. Renew. Energy 95, 367–380. http://dx.doi.org/10.1016/j.renene.2016.04.030.

Fathy, A., Kaaniche, K., Alanazi, T.M., 2020. Recent approach based social spider optimizer for optimal sizing of hybrid PV/Wind/Battery/Diesel integrated microgrid in Aljouf region. IEEE Access 8, 57630–57645. http://dx.doi.org/10.1109/ACCESS.2020.2982805.

Food and Agriculture Organization of the United Nations, 2017. BEFS ASSESSMENT for EGYPT: Sustainable Bioenergy Options from Crop and Livestock Residues. ISBN: 9789251095874.

Gao, Z., Zhao, J., Li, S., Hu, 2020. The improved mayfly optimization algorithm the improved mayfly optimization algorithm. J. Phys. Conf. Ser. 1684, 012077. http://dx.doi.org/10.1088/1742-6596/1684/1/012077.

Geleta, D.K., Manshahia, M.S., Vasant, P., Banik, A., 2020. Grey wolf optimizer for optimal sizing of hybrid wind and solar renewable energy system. Comput. Intell. 1–30. http://dx.doi.org/10.1111/coin.12349.

Gharibi, M., Askarzadeh, A., 2019. Technical and economical bi-objective design of a grid-connected photovoltaic/diesel generator/fuel cell energy system. Sustain. Cities Soc. 50, 101575. http://dx.doi.org/10.1016/j.scs.2019.101575.

Ghosh, S., Karar, V., 2018. Assimilation of optimal sized hybrid photovoltaic-biomass system by dragonfly algorithm with grid. Energies 11, http://dx.doi.org/10.3390/en11071892.

Guo, X., Yan, X., Jermsittiparsert, K., 2021. Using the modified mayfly algorithm for optimizing the component size and operation strategy of a high temperature PEMFC-powered CCHP. Energy Rep. 7, 1234–1245. http://dx.doi.org/10.1016/j.egyr.2021.02.042.

Hadidian Moghaddam, M.J., Kalam, A., Nowdeh, S.A., Ahmadi, A., Babanezhad, M., Saha, S., 2019. Optimal sizing and energy management of stand-alone hybrid photovoltaic/wind system based on hydrogen storage considering LOEE and LOLE reliability indices using flower pollination algorithm. Renew. Energy 135, 1412–1434. http://dx.doi.org/10.1016/j.renene.2018.09.078.

Hassan, H.B.A., el Gebaly, M.R., Ghani, S.S.A., Hussein, Y.M.M., 2014. An economic study of recycling agricultural wastes in Egypt. Middle East J. Agric. Res. 3, 592–608.

Jamshidi, M., Askarzadeh, A., 2019. Techno-economic analysis and size optimization of an off-grid hybrid photovoltaic, fuel cell and diesel generator system. Sustain. Cities Soc. 44, 310–320. http://dx.doi.org/10.1016/j.scs.2018.10.021.

Kashefi Kaviani, A., Riahy, G.H., Kouhsari, S.M., 2009. Optimal design of a reliable hydrogen-based stand-alone wind/PV generating system, considering component outages. Renew. Energy 34, 2380–2390. http://dx.doi.org/10.1016/j.renene.2009.03.020.

Khan, A., Javaid, N., 2020. Optimal sizing of a stand-alone photovoltaic, wind turbine and fuel cell systems. Comput. Electr. Eng. 85, http://dx.doi.org/10.1016/j.compeleceng.2020.106682.

Kharrich, M., Kamel, S., Abdeen, M., Mohammed, O.H., Akherraz, M., Khurshaid, T., Rhee, S.B., 2021a. Developed approach based on equilibrium optimizer for optimal design of hybrid PV/Wind/Diesel/Battery microgrid in Dakhla, Morocco. IEEE Access 9, 13655–13670. http://dx.doi.org/10.1109/ACCESS.2021.3051573.

Kharrich, M., Mohammed, O.H., Alshammari, N., Akherraz, M., 2021b. Multi-objective optimization and the effect of the economic factors on the design of the microgrid hybrid system. Sustain. Cities Soc. 65, 102646. http://dx.doi.org/10.1016/j.scs.2020.102646.

Li, J., Liu, P., Li, Z., 2020. Optimal design and techno-economic analysis of a solar-wind-biomass off-grid hybrid power system for remote rural electrification: A case study of west China. Energy 208, 118387. http://dx.doi.org/10.1016/j.energy.2020.118387.

Maleki, A., Nazari, M.A., Pourfayaz, F., 2020. Harmony search optimization for optimum sizing of hybrid solar schemes based on battery storage unit. Energy Rep. http://dx.doi.org/10.1016/j.egyr.2020.03.014.

Maleki, A., Pourfayaz, F., 2015. Sizing of stand-alone photovoltaic/wind/diesel system with battery and fuel cell storage devices by harmony search algorithm. J. Energy Storage 2, 30–42. http://dx.doi.org/10.1016/j.est.2015.05.006.

Mills, A., Al-Hallaj, S., 2004. Simulation of hydrogen-based hybrid systems using Hybrid2. Int. J. Hydrogen Energy 29, 991–999. http://dx.doi.org/10.1016/j.ijhydene.2004.01.004.

Mirjalili, S., 2016. SCA: A Sine cosine algorithm for solving optimization problems. Knowledge-Based Syst. 96, 120–133. http://dx.doi.org/10.1016/j.knosys.2015.12.022.

Mirjalili, S., Lewis, A., 2016. The whale optimization algorithm. Adv. Eng. Softw. 95, 51–67. http://dx.doi.org/10.1016/j.advengsoft.2016.01.008.

Naderipour, A., Abdul-Malek, Z., Zahedi Vahid, M., Mirzaei Seifabad, Z., Hajivand, M., Arabi-Nowdeh, S., 2019. Optimal, reliable and cost-effective framework of photovoltaic-wind-battery energy system design considering outage concept using grey wolf optimizer algorithm - Case study for Iran. IEEE Access 7, 182611–182623. http://dx.doi.org/10.1109/ACCESS.2019.2958964.

Ray, M., Sheeran, R., Lewis, E., Cavanagh, J., 2007. The climate change Levy and climate change agreements a review by the national audit office. Natl. Audit Off..

Samy, M.M., Barakat, S.H., 2020. Biomass and fuel cells multi-objective optimization of hybrid renewable energy system based on biomass and fuel cells. http://dx.doi.org/10.1002/er.5815.

Sanajaoba, S., 2019. Optimal sizing of off-grid hybrid energy system based on minimum cost of energy and reliability criteria using firefly algorithm. Sol. Energy 188, 655–666. http://dx.doi.org/10.1016/j.solener.2019.06.049.

Shi, R., Wang, W., Yuan, Z., Fan, X., Ramezani, S., 2021. A novel optimum arrangement for a hybrid renewable energy system using developed student psychology based optimizer: A case study. Energy Rep. 7, 70–80. http://dx.doi.org/10.1016/j.egyr.2020.11.168.

Singh, A., Baredar, P., 2016. Techno-economic assessment of a solar PV, fuel cell, and biomass gasifier hybrid energy system. Energy Rep. 2, 254–260. http://dx.doi.org/10.1016/j.egyr.2016.10.001.

Singh, S., Kaushik, S.C., 2016. Optimal sizing of grid integrated hybrid PV-biomass energy system using artificial bee colony algorithm. IET Renew. Power Gener. 10, 642–650. http://dx.doi.org/10.1049/iet-rpg.2015.0298.

Sultan, H.M., Kuznetsov, O.N., Menesy, A.S., Kamel, S., 2020. Optimal configuration of a grid-connected hybrid PV/Wind/Hydro-Pumped storage power system based on a novel optimization algorithm. In: Proc. 2nd 2020 Int. Youth Conf. Radio Electron. Electr. Power Eng.. REEPE 2020, http://dx.doi.org/10.1109/REEPE49198.2020.9059189.

Sultan, H.M., Menesy, A.S., Kamel, S., Korashy, A., Almohaimeed, S.A., Abdel-Akher, M., 2021. An improved artificial ecosystem optimization algorithm for optimal configuration of a hybrid PV/WT/FC energy system. Alexandria Eng. J. 60, 1001–1025. http://dx.doi.org/10.1016/j.aej.2020.10.027.

Suresh, M., Meenakumari, R., 2019. An improved genetic algorithm-based optimal sizing of solar photovoltaic/wind turbine generator/diesel generator/battery connected hybrid energy systems for standalone applications. Int. J. Ambient Energy 1–20. http://dx.doi.org/10.1080/01430750.2019.1587720.

Tabak, A., Kayabasi, E., Guneser, M.T., Ozkaymak, M., 2019. Grey wolf optimization for optimum sizing and controlling of a PV/WT/BM hybrid energy system considering TNPC, LPSP, and LCOE concepts. Energy Sources, Part A Recover. Util. Environ. Eff. 1–21. http://dx.doi.org/10.1080/15567036.2019.1668880.

Vendoti, S., Muralidhar, M., Kiranmayi, 2021. Techno-economic analysis of off-grid solar/wind/biogas/biomass/fuel cell/battery system for electrification in a cluster of villages by HOMER software. Environ. Dev. Sustain. 23, 351–372. http://dx.doi.org/10.1007/s10668-019-00583-2.

Wang, Y., Chen, K.S., Mishler, J., Cho, S.C., Adroher, X.C., 2011. A review of polymer electrolyte membrane fuel cells: Technology, applications, and needs on fundamental research. Appl. Energy 88, 981–1007. http://dx.doi.org/10.1016/j.apenergy.2010.09.030.

Wang, Y., Seo, B., Wang, B., Zamel, N., Jiao, K., Adroher, X.C., 2020. Fundamentals, materials, and machine learning of polymer electrolyte membrane fuel cell technology. Energy AI 1, 100014. http://dx.doi.org/10.1016/j.egyai.2020.100014.

Wolpert, D.H., Macready, W.G., 1997. No free lunch theorems for optimization. IEEE Trans. Evol. Comput. 1, 67–82.

Zervoudakis, K., Tsafarakis, S., 2020. A mayfly optimization algorithm. Comput. Ind. Eng. 145, http://dx.doi.org/10.1016/j.cie.2020.106559.